PL-TR-95-2061

PRISM: A PARAMETERIZED REAL-TIME IONOSPHERIC SPECIFICATION MODEL, VERSION 1.5

R. E. Daniell, Jr.
L. D. Brown

Computational Physics, Inc.,
385 Elliot Street
Newton, MA 02164

31 May 1995

Final Report
19 February 1992 – 31 March 1995

Approved for public release; distribution unlimited

PHILLIPS LABORATORY
DIRECTORATE OF GEOPHYSICS
AIR FORCE MATERIEL COMMAND
HANSCOM AIR FORCE BASE, MASSACHUSETTS 01731-3010

"This technical report has been reviewed and is approved for publication"

Signature
CHRISTOPHER SHERMAN
Contract Manager

Signature
DAVID ANDERSON
Branch Chief

Signature
WILLIAM K. VICKERY
Division Director

This report has been reviewed by the ESC Public Affairs Office (PA) and is releasable to the National Technical Information Service (NTIS).

Qualified requestors may obtain additional copies from the Defense Technical Information Center (DTIC). All others should apply to the National Technical Information Service (NTIS).

If your address has changed, if you wish to be removed from the mailing list, or if the addressee is no longer employed by your organization, please notify PL/TSI, 29 Randolph Road, Hanscom AFB, MA 01731-3010. This will assist us in maintaining a current mailing list.

Do not return copies of this report unless contractual obligation or notices on a specific document requires that it be returned.

REPORT DOCUMENTATION PAGE

Form Approved
OMB No. 0704-0188

1. AGENCY USE ONLY (*Leave blank*)	2. REPORT DATE	3. REPORT TYPE AND DATES COVERED
	31 May 1995	Final Report (19 Feb 92 - 31 Mar 95)

4. TITLE AND SUBTITLE
PRISM: A Parameterized Real-Time Ionospheric Specification Model, Version 1.5

5. FUNDING NUMBERS
PE63707F
PR 4026 TA01 WULA

Contract F19628-92-C-0044

6. AUTHOR(S)
Robert E. Daniell, Jr., & Lincoln D. Brown

7. PERFORMING ORGANIZATION NAME(S) AND ADDRESS(ES)
Computational Physics, Inc.
Suite 202A
240 Bear Hill Road
Waltham, MA 02154

8. PERFORMING ORGANIZATION REPORT NUMBER

9. SPONSORING / MONITORING AGENCY NAME(S) AND ADDRESS(ES)
Phillips Laboratory
29 Randolph Road
Hanscom AFB, MA 01731-3010
Contract Manager: Christopher Sherman/GPIM

10. SPONSORING / MONITORING AGENCY REPORT NUMBER
PL-TR-95-2061

11. SUPPLEMENTARY NOTES

12A. DISTRIBUTION / AVAILABILITY STATEMENT
APPROVED FOR PUBLIC RELEASE;
DISTRIBUTION UNLIMITED

12b. DISTRIBUTION CODE

13. ABSTRACT (*Maximum 200 words*)

This report describes PRISM Version 1.5, a parameterized, real-time ionospheric specification model. PRISM was developed for use at the Air Force Space Forecast Center (50th Weather Squadron) at Falcon Air Force Base. PRISM consists of the theoretical climatology model, PIM (Parameterized Ionospheric Model), and an algorithm for updating PIM electron density profiles using ground based and spaced data. PIM is based on a set of diurnally reproducible runs of theoretical ionospheric models for a broad range of geophysical conditions and for three seasons (June, December, and March/September). PRISM is capable of ingesting and utilizing data from digital or analog ionosondes, polarimeter or GPS based TEC measurements, in situ plasma measurements (electron density, electron temperature, ion composition, ion temperature, and plasma drift velocity), and auroral electron and ion precipitation measurements. PRISM 1.5 contains a number of improvements over PRISM 1.0, which was described in PL-TR-91-2299, including improved climatology, improved handling of in situ plasma data, and the ability to ingest and utilize TEC data.

14. SUBJECT TERMS
ionosphere, space environment, space weather, ionospheric specification

15. NUMBER OF PAGES
78

16. PRICE CODE

17. SECURITY CLASSIFICATION OF REPORT	18. SECURITY CLASSIFICATION OF THIS PAGE	19. SECURITY CLASSIFICATION OF ABSTRACT	20. LIMITATION OF ABSTRACT
Unclassified	Unclassified	Unclassified	SAR

Table of Contents

List of Figures

List of Tables

Executive Summary

We describe the development of PRISM (*P*arameterized *R*eal-time *I*onospheric *S*pecification *M*odel), a global near real-time ionospheric specification model intended for use at the Air Force Space Forecast Center (AFSFC), also known as the 50th Weather Squadron (50 WS). We also describe PIM (*P*arameterized *I*onospheric *M*odel), the base ionospheric model which forms the core of PRISM. PIM consists of a semi-analytic representation of a parameterization of four separate physically based computational models of the ionosphere. PRISM uses both ground based and space based data to modify or update the PIM ion density profiles to produce a data driven specification of the state of the ionosphere. At AFSFC PRISM will provide hourly ionospheric specifications in near real time. PRISM is capable of accepting and using bottomside electron density profiles produced from automated true height analysis of digital ionograms, TEC measurements from GPS receivers, satellite based *in situ* plasma measurements (electron density, ion composition, electron and ion temperature, and ion drift velocity), satellite based *in situ* observations of precipitating electrons and ions in the high latitude regions, as well as ionospheric parameters derived from observations of airglow and auroral optical emissions. We describe the construction of PIM, and the real time adjustment process of PRISM, as implemented in Version 1.5. This is the version that will become operational at AFSFC in the fall of 1995.

1. INTRODUCTION

We have developed a Parameterized Real-time Ionospheric Specification Model (PRISM) for the Air Force Air Weather Service (AFAWS) for use at the Air Force Space Forecast Center (AFSFC, also known as the 50th Weather Squadron). The model uses both ground based and space based data available in near real time to modify a Parameterized Ionospheric Model (PIM) and thus provide a near real-time specification of the ionosphere. PIM is a composite of diurnally reproducible runs of several physical ionospheric models: (1) the Time Dependent Ionospheric Model (TDIM) of Utah State University (USU) [*Schunk*, 1988], (2) the low latitude F-region model (LOWLAT) developed by *Anderson* [1973], (3) the midlatitude version of LOWLAT (called MIDLAT) developed by D. N. Anderson and modified by D. T. Decker, and (4) an E-region local chemistry code developed by D. T. Decker and incorporating photoelectrons using the continuous slowing down method [*Jasperse*, 1982].

Both PIM and PRISM can produce either regional or global output. The output grid of latitude and longitude (which may be either geographic or geomagnetic) is user selectable. At AFSFC the standard PRISM output is a global grid with 1° latitude spacing and 5° longitude spacing. Profile parameters (f_oF_2, h_mF_2, TEC, etc.), or complete electron density profiles, or both may be output to the specified grid.

PRISM has been delivered to the AFAWS and is presently undergoing transition to operational code. PIM is in the public domain and is available for distribution to the ionospheric community. PRISM is also available to the research community upon application to the AFAWS. PIM has been distributed to about 60 users worldwide. PRISM is in use by three research groups in the United States.

1.1 *Objectives*

Our primary objective was the development of an algorithm for using near real time satellite and ground based data to provide a near real time specification of the global ionosphere. The data to be used include

(1) bottomside digital soundings from the AFAWS Digital Ionospheric Sounding System (DISS),
(2) Total Electron Content (TEC) data from the AFAWS Transionospheric Sensing System (TISS),
(3) in situ plasma data (densities, temperatures, and drift velocities) from the SSIES instrument on DMSP satellites,
(4) auroral electron and ion fluxes from the SSJ/4 instrument on DMSP satellites, and
(5) electron density profile information deduced from observations of airglow and auroral optical emissions by instruments (SSUSI and SSULI) expected to be flown on future DMSP satellites.

The need for a global specification of the state of the ionosphere is twofold. First, there are operational systems that need to correct for ionospheric effects in real time, or that have operational parameters that are affected by the ionosphere and must be adjusted in near real time. Second, the operation of many systems could be optimized if accurate forecasts of ionospheric conditions were available because this allows the operational parameters to be chosen ahead of time. Any ionospheric forecast algorithm will require an accurate specification of the current state of the ionosphere as an initial condition, which PRISM provides.

In addition to real time needs, many system operators need post-event analysis to determine whether operational problems or outages were caused by system problems or by environmental conditions. PRISM will be used for this purpose at AFSFC as well.

1.2 *Approach*

Ideally, the specification of the current state of the ionosphere would be obtained directly from real time observations from a dense network of satellite and ground based instruments. Unfortunately, the complexity and spatial extent of the ionosphere precludes the deployment of a sufficiently dense network of observing instruments. Therefore, any practical ionospheric

specification algorithm must be based on an ionospheric model with parameters that can be adjusted on the basis of near real time data. Two approaches are possible: (1) statistical or empirical climatological models or (2) numerical simulations based on physical models. (In this paper "physical model" is synonymous with "numerical model.") For reasons described below, we have chosen the second approach (physical models). However, practical considerations (primarily computational speed) dictate that the algorithms implemented at the Space Forecast Center be based on *parameterized* versions of the physical models ("theoretical climatology").

We feel strongly that a comprehensive physical model of ionospheric processes can produce more accurate specifications and forecasts than can statistical or climatological models. The causal relationship between easily monitored solar and geophysical parameters (e.g., K_p, $F_{10.7}$, etc.) and a particular ionospheric configuration is very complex. Any organization of historical ionospheric data inevitably averages over a variety of ionospheric configurations corresponding to similar values of the chosen set of solar-geophysical parameters (usually only one or two). The result is that spatial structure tends to be smeared out or smoothed over, and the resulting model is unrepresentative of the *instantaneous* ionosphere. If a physical model contains all of the relevant physics, and if the inputs are realistic, then it will produce more realistic representations of instantaneous ionospheric structure. However, there is a difference between a *realistic* representation and an *accurate* one.

In order to accurately simulate a time dependent phenomenon like the ionosphere, a physical model needs an accurate specification of the initial conditions and an accurate representation of the energy and momentum flux at the boundaries. For the purposes of providing a specification model, it is the energy and momentum input that is crucial. If the model is run long enough, the effects of the initial conditions are lost and the present state of the model depends only on the recent history of the energy and momentum input. These include the solar EUV (the primary source of ionization outside the auroral zone), high latitude heating of the thermosphere (which affects the global circulation of the thermosphere), high latitude convection, and low latitude dynamo electric fields. While the temporal and spatial resolution of the observations of these quantities are expected to improve in the future, they will probably never be sufficient to

allow accurate simulation of the ionosphere without additional data. As a practical matter, ionospheric simulations must be, and will remain, iterative in nature: The energy and momentum input parameters are adjusted until the simulation agrees with observations of ionospheric parameters to some level of accuracy.

A practical consequence of this situation is that the production of an accurate ionospheric specification based on a numerical simulation requires that the physical model be run several (perhaps many) times until its output agrees with the available observations. The requirement that the model cover a sufficient time period to allow the transient effects of the initial conditions to damp out implies that the physical model must run much faster than the system it is simulating. At the present time, given practical (i.e., financial) limits on the available computing power, this is not possible. Consequently, we have adopted a modified approach in which the physical models are parameterized in terms of solar and geophysical parameters. It is these parameterized models rather than the original physical models which are to be adjusted according to the real time ionospheric data.

There is a superficial similarity between our approach and a climatological approach. The difference, however, is that we begin with a more realistic representation of the spatial structure of the ionosphere than climatological models can provide. The parameter adjustment process should not compromise this advantage. In the future, as more powerful computers and more efficient model algorithms become available, the parameterized models can be replaced by actual physical models to produce more accurate specifications.

2. THE PHYSICAL MODELS

Four separate physical models were used as the basis of PRISM: (1) a low latitude F layer model (LOWLAT), (2) a midlatitude F layer model (MIDLAT), (3) a combined low and middle latitude E layer model (ECSD), and (4) a high latitude E and F layer model (TDIM). All four models are based on a tilted dipole representation of the geomagnetic field and a corresponding magnetic coordinate system. (Hereafter, "latitude" means "magnetic latitude" unless otherwise noted.) All four models use the MSIS-86 neutral atmosphere model [*Hedin*, 1987]. Chemical reaction rates, collision frequencies, and similar data are consistent among all the models.

2.1 *The Low Latitude F Layer Model*

The low latitude *F* region model (LOWLAT) was originally developed by *Anderson*, [1973]. (See also *Moffett*, [1979]). It solves the diffusion equation for O^+ along a magnetic flux tube. Normally, the entire flux tube is calculated with chemical equilibrium boundary conditions at both feet of the flux tube. A large number of flux tubes must be calculated in order to build up an altitude profile.

Since heat transport is not included in this model, ion and electron temperature models must be used. For the PRISM development effort we chose the temperature model of *Brace and Theis* [1981]. The Horizontal Wind Model (HWM) of *Hedin* [1988] was used to describe thermospheric winds.

The critical feature incorporated in the low latitude model is the dynamo electric field. The horizontal component of this field drives upward convection through $\mathbf{E}\times\mathbf{B}$ drift, and this can significantly modify profile shapes and densities. This phenomenon is responsible for the equatorial anomaly, crests in ionization on either side of the magnetic equator at $\pm 15-20°$ magnetic latitude. In the current version of PRISM (Version 1.5) the $\mathbf{E}\times\mathbf{B}$ driven vertical drift used for these calculations was based on the empirical models derived from data from the Atmospheric Explorer-E (AE-E) satellite [*Fejer et al.*, 1995], which are consistent with the drifts measured at Jicamarca [*Fejer*, 1981; *Fejer et al.*, 1989] but include longitudinal variations as well. We used the *Fejer et al.* [1995] empirical drifts for moderate and high solar activity. Following

the their discussion, we modified these drifts by reducing or eliminating the pre-reversal enhancement for low solar activity. Horizontal drifts were neglected in the PRISM runs.

Since its original development this model has undergone extensive validation by comparison with data. The most recent such comparison is *Preble et al.* [1994] using electron density profiles measured by the incoherent scatter radar facility at Jicamarca, Peru.

2.2 *The Midlatitude F Layer Model*

The midlatitude *F* region model (MIDLAT) is the same as the low latitude version, except that the dynamo electric field is not included. Complete flux tubes are followed, but neither horizontal nor vertical convection is included. The computer resource requirements of MIDLAT are far less than those of LOWLAT. As long as the boundary between low and middle latitudes is chosen so that the electric field is negligible on the boundary flux tubes, the two models give identical results at the boundary ensuring continuity across that boundary. For the PRISM development effort we used the same temperature model [*Brace and Theis*, 1981] and the same thermospheric wind model [*Hedin*, 1988]. For appropriate production, loss, and diffusion rates for both LOWLAT and MIDLAT, see *Decker et al.* [1994].

2.3 *The Low and Midlatitude E Layer Model*

The low and mid- latitude *E* region model (ECSD) was developed by Dwight T. Decker and John R. Jasperse and incorporates photoelectrons calculated using the continuous slowing down (CSD) approximation [*Jasperse*, 1982]. Ion concentrations are calculated assuming local chemical equilibrium. A small nighttime source is included to ensure that an E layer is maintained throughout the night.

2.4 *The High Latitude Model*

The high latitude model (incorporating both E and F layers) is the Utah State University (USU) Time Dependent Ionospheric Model (TDIM). (See *Schunk* [1988] for a review.) This model is similar to the low and middle latitude models except that the flux tubes are truncated and a flux boundary condition is applied at the top. In addition, the flux tubes move under the influence of the high latitude convection electric field. In the low latitudes, because the magnetic field is mainly horizontal, the effect of the electric field is primarily to move the ionization in altitude. In contrast, the high latitude magnetic field is mainly vertical, and the electric field driven convection is horizontal. Like LOWLAT, this model has a long history and has been validated by numerous comparisons with data.

TDIM includes an E-layer model that incorporates the effects of ionization by precipitating auroral particles. The ion production rates used were calculated using the B3C electron transport code [*Strickland*, 1976; *Strickland et al.*, 1994] and incident electron spectra representative of DMSP SSJ/5 data. The characteristics of the electron spectra were taken from the *Hardy et al.* [1987] electron precipitation model. The high latitude convection patterns were those developed by *Heppner and Maynard* [1987] for southward directed B_z.

3. PARAMETERIZATION OF THE PHYSICAL MODELS

Parameterization of the physical models proceeded in two steps. First, the models were used to generate a number of "databases" for a discrete set of geophysical conditions. Each database consists of ion density profiles on a discrete grid of latitudes and longitudes for a 24 hour period in UT. Second, to reduce storage requirements, the databases were approximated with semi-analytic functions. These two processes are described in the following subsections.

3.1 *Geophysical Parameters*

All the physical models were parameterized in terms of season and solar activity. The middle and high latitude models were also parameterized in terms of magnetic activity, while the high latitude model was additionally parameterized in terms of the sign of the interplanetary magnetic field component B_y. (The high latitude model was only run using B_z southward. Northward B_z conditions are modeled using the low magnetic activity databases.) For the middle and low latitudes, the F layer (O^+) and the E layer (NO^+ and O_2^+) were computed and parameterized separately. The high latitude model (TDIM) produced all three ions simultaneously.

Due to time and computer resource limitations, only a few values of each parameter were used. The season "values" are the June and December solstices and the March equinox (which also "stands in" for the September equinox). We expect to change from seasonal to monthly values in the next versions of PIM and PRISM. The values of the other parameters are summarized for each latitude region in Table 1. Note that the USU TDIM and LOWLAT produce output in magnetic local time (MLT), while MIDLAT and ECSD produce output in magnetic longitude. Since the two coordinates are readily interconvertible, we will ignore the distinction and refer only to magnetic longitude in the description that follows.

Table 1: Geophysical Parameter Values

	Solar Activity ($F_{10.7}$)	Magnetic Activity (K_p)	IMF B_y direction	Number of databases
Low Latitude F layer	70, 130, 210	N/A	N/A	36[a]
Midlatitude F layer	70, 130, 210	1, 3.5, 6	N/A	54[b]
Low & Midlatitude E layer	70, 130, 210	1, 3.5, 6	N/A	54[c]
High Latitude E & F layer	70, 130, 210	1, 3.5, 6	+, -	324[d]

[a] 3 seasons × 3 solar activities × 4 longitude sectors

[b] 3 seasons × 3 solar activities × 3 magnetic activities × 2 hemispheres

[c] 3 seasons × 3 solar activities × 3 magnetic activities × 2 species

[d] 3 seasons × 3 solar activities × 3 magnetic activities × 2 By's × 3 species × 2 hemispheres

3.2 *Representation of the Databases*

When the models are run for any one set of geophysical parameters (e.g., June, $F_{10.7} = 130$, $K_p = 1$), they produce ion densities (O^+, NO^+, and O_2^+) on a four dimensional grid. MIDLAT and ECSD use a grid of magnetic latitude (λ), magnetic longitude (φ), altitude(z), and Universal Time (τ). TDIM uses magnetic local time (MLT or ψ) instead of magnetic longitude, while LOWLAT uses MLT instead of UT. In order to make this mass of numbers more manageable, we produced a semi-analytical representation of each database. The space and time grid parameters are summarized for each latitude region in Table2.

Due to the computer resource requirements of the low latitude F layer code, it was used to generate databases at four discrete longitudes (corresponding to longitude sectors for which **E×B** drift measurements were available). Each longitude sector was parameterized separately, and the necessary longitude interpolation is carried out in PIM and PRISM during execution, as described below.)

Because we were trying to represent discrete data (rather than continuous functions), and because we were working with regional rather than global data sets, we felt that the usual spherical harmonic expansion techniques were not appropriate. Instead we concentrated on the use of orthogonal functions of discrete variables.

Table 2: Horizontal Grid Parameters

Latitude Region	Magnetic Latitude	Magnetic Longitude	UT	Number of altitude profiles per database
Low Latitude F layer	−32° to 32° in 2° steps	30°, 149°, 250°, and 329°	MLT: 0.0 to 23.5 in 0.5 hr steps	1,584
Midlatitude F layer	30° to 74° and −30° to −74° in 4° steps	0° to 345° in 15° steps	0100 to 2300 in 2 hr steps	3,456
Low and Midlatitude E layer	−76° to 76° in 4° steps	0° to 345° in 15° steps	0100 to 2300 in 2 hr steps	11,232
High Latitude E & F layer	51° to 89° and −51° to −89° in 2° steps	MLT: 0.5 to 23.5 in 1 hour steps	0100 to 2300 in 2 hr steps	5,760

We considered the use of modified Chapman functions for representing altitude profiles of ion densities. These functions have the advantage that peak height and peak density are explicit parameters, but the extremely non-linear nature of these functions necessitates the use of non-linear least squares fitting methods. While such methods produced excellent representations of individual profiles, the variation of the fitted parameters with latitude, longitude (or MLT), and UT was unacceptably noisy. Consequently, we chose to use Empirical Orthornormal Functions for the altitude representation.

Empirical Orthonormal Functions (EOFs) have been used extensively to represent meteorological and climatological data [*Lorenz*, 1956; *Kutzbach*, 1967; *Davis*, 1976; and *Peixota and Oort*, 1991]. They have also been used for empirical ionospheric modeling [*Secan and Tascione*, 1984]. EOFs are described in Appendix A. They have the advantage of providing a representation in terms of linear combinations of orthogonal functions, which allows for straightforward determination of coefficients. However, because peak density and peak height are not explicit parameters of the representation, these parameters can be determined only by reconstructing the entire profile and invoking a peak finding algorithm. We expect to revisit this problem in future versions of PIM and PRISM and implement a new representation that combines

the attractive features of both methods, i.e., that includes peak density and peak height as explicit parameters yet relies on linear combinations of orthogonal functions to describe the profile shape.

For longitude (or local time) variations (and for the low latitude F layer UT variation), the obvious choice is a Fourier series, since trigonometric functions retain their orthogonality properties on uniform discrete grids and because the data is periodic in the independent variable. These worked quite well for the high latitude models under all conditions and for the low and midlatitude models under low to moderate solar activity conditions. However, they did not work well for the low and midlatitude models under high solar activity conditions, apparently because the EOF coefficients exhibited exceptionally large gradients at dawn and dusk. Therefore, we decided to tabulate the coefficients in longitude for all the low and midlatitude databases.

For the latitude variations, we chose to generate grid-specific orthogonal polynomials using the algorithm derived in *Beckmann* [1973] and described in Appendix B. To help keep the notation straight, we summarize it in Table3.

Table 3. Notation Summary

grid	variable	index	orthogonal function	index
altitude	z_i	$1 \le i \le I$	EOF: $g_m(z_i)$	$1 \le m \le M$
latitude	λ_j	$1 \le j \le J$	polynomial: $u_n(\lambda)$	$0 \le n \le N$
longitude	φ_k	$1 \le k \le K$	trigonometric[a]: $\cos(p\varphi)$ and $\sin(p\varphi)$	$0 \le p \le P$
local time	ψ_k	$1 \le k \le K$	trigonometric[b]: $\cos(p\psi)$ and $\sin(p\psi)$	$0 \le p \le P$
UT	τ_l	$1 \le l \le L$	trigonometric[a]: $\cos(q\tau)$ and $\sin(q\tau)$	$0 \le q \le Q$

[a]Not used for any database in PRISM 1.5, but may be used in future versions.
[b]Used only for high latitude databases.

The semianalytic representation of each database was generated in several steps. For all ionospheric regions, the first step was the determination of the EOFs from the ion densities in the database and a set of coefficients $c_{lm}(\lambda_j, \varphi_k)$ for representing each ion density profile on the latitude, longitude, UT grid (See Appendix A).

$$n_s(z_i,\lambda_j,\psi_k,\tau_l) \approx \sum_{m=1}^{M} c_m^{(s)}(\lambda_j,\psi_k,\tau_l) g_m^{(s)}(z_i) \qquad \text{[TDIM]} \qquad (1a)$$

$$n_s(z_i,\lambda_j,\varphi_k,\tau_l) \approx \sum_{m=1}^{M} c_m^{(s)}(\lambda_j,\varphi_k,\tau_l) g_m^{(s)}(z_i) \qquad \text{[MIDLAT, ECSD]} \qquad (1b)$$

$$n_s(z_i,\lambda_j,\varphi_k,\psi_l) \approx \sum_{m=1}^{M} c_m^{(s)}(\lambda_j,\varphi_k,\psi_l) g_m^{(s)}(z_i) \qquad \text{[LOWLAT]} \qquad (1c)$$

where z_i, λ_j, φ_k, ψ_k, τ_j, and ψ_l are all points on the model output grid, and $g_m^{(s)}(z_i)$ is the m^{th} EOF evaluated at z_i. (Note, however, that a different set of $g_m^{(s)}(z_i)$ functions are used for each ion, for each set of geophysical conditions, and for each model.)

For the high latitude model (TDIM, both *E*- and *F*-layers), the second step was the generation of Fourier coefficients in MLT, $a_{mp}^{(s)}(\lambda_j,\tau_l)$ and $b_{mp}^{(s)}(\lambda_j,\tau_l)$, for each point on the latitude, UT grid.

$$n_s(z_i,\lambda_j,\psi,\tau_l) \approx \sum_{m=1}^{M}\sum_{p=0}^{P}\left\{a_{mp}^{(s)}(\lambda_j,\tau_l)\cos(p\psi)+b_{mp}^{(s)}(\lambda_j,\tau_l)\sin(p\psi)\right\} g_m^{(s)}(z_i) \qquad \text{[TDIM]} \qquad (2)$$

For the low and midlatitude models, we found that a truncated Fourier series often introduced spurious longitudinal dependences, apparently driven by the steep gradients at dawn and dusk. The effect was particularly pronounced at high solar activity when the day/night contrast is the greatest. Consequently, for these models, the EOF coefficients remain tabulated in longitude.

For all models, the next step was the generation of orthogonal polynomials from the latitude grid (Appendix B). For the high latitude model (TDIM) the coefficients are $\alpha_{mnp}^{(s)}(\tau_l)$ and $\beta_{mnp}^{(s)}(\tau_l)$, and the ion density is approximated by

$$n_s(z_i,\lambda,\psi,\tau_l) \approx \sum_{m=1}^{M}\sum_{n=0}^{N}\sum_{p=0}^{P}\left\{\alpha_{mnp}^{(s)}(\tau_l)\cos(p\psi)+\beta_{mnp}^{(s)}(\tau_l)\sin(p\psi)\right\} g_m(z_i)u_n(\lambda) \qquad \text{[TDIM]} \qquad (3a)$$

For MIDLAT and ECSD the coefficients are $\gamma_{mn}^{(s)}(\lambda_k,\tau_l)$ and the ion density is approximated by

$$n_s(z_i,\lambda,\varphi_k,\tau_l) \approx \sum_{m=1}^{M}\sum_{n=0}^{N}\gamma_{mn}^{(s)}(\varphi_k,\tau_l)g_m(z_i)u_n(\lambda) \qquad \text{[MIDLAT, ECSD]} \qquad (3b)$$

For LOWLAT the coefficients are $\eta_{mn}^{(s)}(\varphi_k,\psi_l)$ and the ion density is approximated by

$$n_s(z_i,\lambda,\varphi_k,\psi_l) \approx \sum_{m=1}^{M}\sum_{n=0}^{N}\eta_{mn}^{(s)}(\varphi_k,\psi_l)g_m(z_i)u_n(\lambda) \qquad \text{[LOWLAT]} \qquad (3c)$$

The number of terms in each series are listed in Table4 for each region.

Table 4: Altitude Grids and EOF's

Database	number of altitude points	minimum altitude	maximum altitude	number of EOF's
low latitude O^+	55	160	1600	9
midlatitude O^+	49	125	1600	8
low & midlatitude NO^+ & O_2^+	28	90	400	7
high latitudeO^+, NO^+, & O_2^+	37	100	800	6

Note that in none of these cases was the altitude spacing uniform.

Because of the extensive use of tabulated coefficients, the ion density at an arbitrary point must be obtained by interpolation. In PIM and PRISM, altitude interpolation is quadratic, while UT interpolation is linear. For the MIDLAT databases, the longitude interpolation is also linear, as is the local time interpolation in the LOWLAT databases. However, the longitude interpolation in the LOWLAT databases is more complicated. First, the O^+ profile for the desired magnetic latitude and local time is reconstructed for each of the four longitude sectors. Then the peak height and peak density is determined for each profile. The peak height for the desired longitude is determined by Fourier interpolation, and all four profiles are shifted to match the interpolated peak height. Then Fourier interpolation is used at each altitude to obtain the interpolated ion density profile.

3.3 *Merging the Regional Models*

Because we used four different regional models in the development of PRISM, the models must be merged at region boundaries. Specifically, the low latitude and midlatitude O^+ models have to be merged across the boundary between low and middle latitudes, while all three ions (O^+, NO^+, and O_2^+) must be merged across the boundary between midlatitudes and high latitudes.

The transition from low latitude O^+ profiles to midlatitude O^+ profiles takes place between 30° and 34° in both hemispheres. The transition is accomplished by taking a weighted average of the h_mF_2 values from the two models in which the weight shifts linearly from 100% low latitude at 30° to 100% midlatitude at 34°. The profiles are shifted to match the averaged h_mF_2 values and then a similar weighted average of the shifted profiles is taken to produce the final merged profile. No transition for NO^+ and O_2^+ is necessary since a single model was used for these ions.

The transition from midlatitude to high latitude takes place over an 8° wide zone whose poleward boundary is the equatorward boundary of the trough. The transition process is similar to the low to midlatitude transition, except that the high latitude profiles are shifted to match the h_mF_2 and h_mE values given by the midlatitude models. The final profile is produced by a weighted average of midlatitude and (shifted) high latitude profiles.

Although PIM and PRISM use geomagnetic coordinates internally, they can produce output in either geomagnetic or geographic coordinates. A contour map of N_mF_2 in geographic coordinates (cylindrical projection) for the June solstice at high solar activity and moderate magnetic activity is displayed in Figure 1. The equatorial anomaly is clearly visible between East longitudes 30° and 180°, corresponding to local times of 1400 and 2400. The high latitude is more clearly seen in a polar projection such as is displayed in Figure 2, again in geographic coordinates. The figure shows the northern hemisphere at the December solstice. B_y is positive, and the tongue of ionization resulting from a steady convection pattern is clearly visible on the evening side.

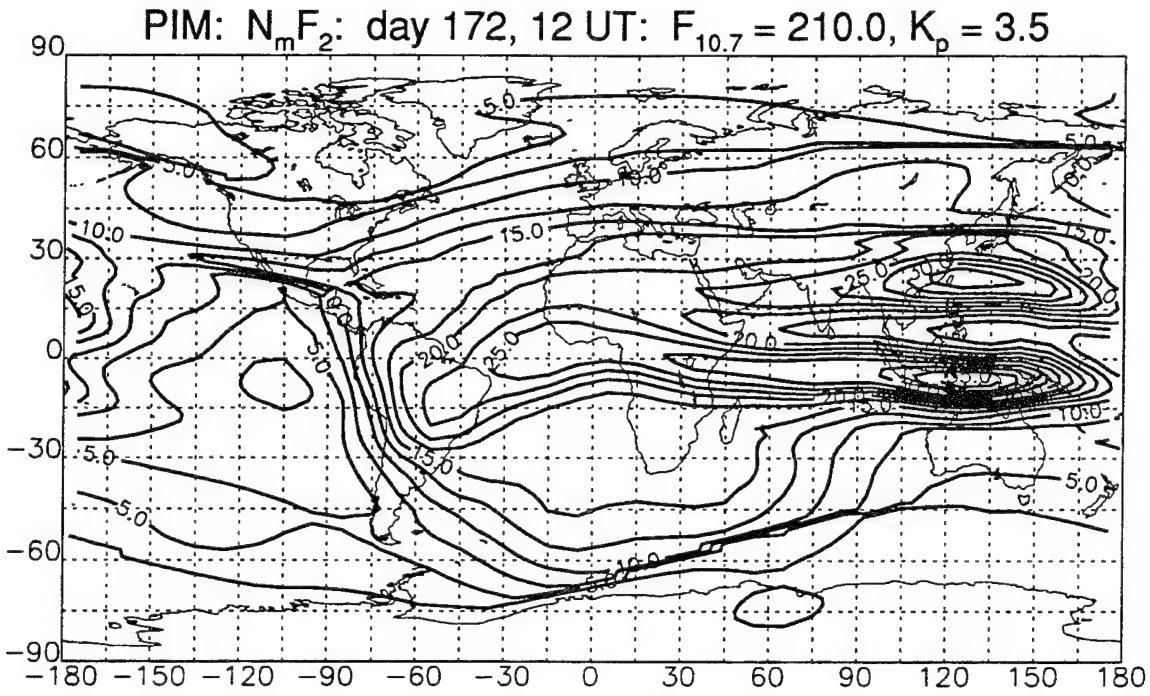

Figure 1. Contours of N_mF_2 (in units of 10^5 cm^{-3}) in cylindrical equidistant projection from PIM for high solar activity, moderate magnetic activity, at 12 UT near the June solstice. The equatorial anomaly is clearly evident from about 1400 to 2400 local time.

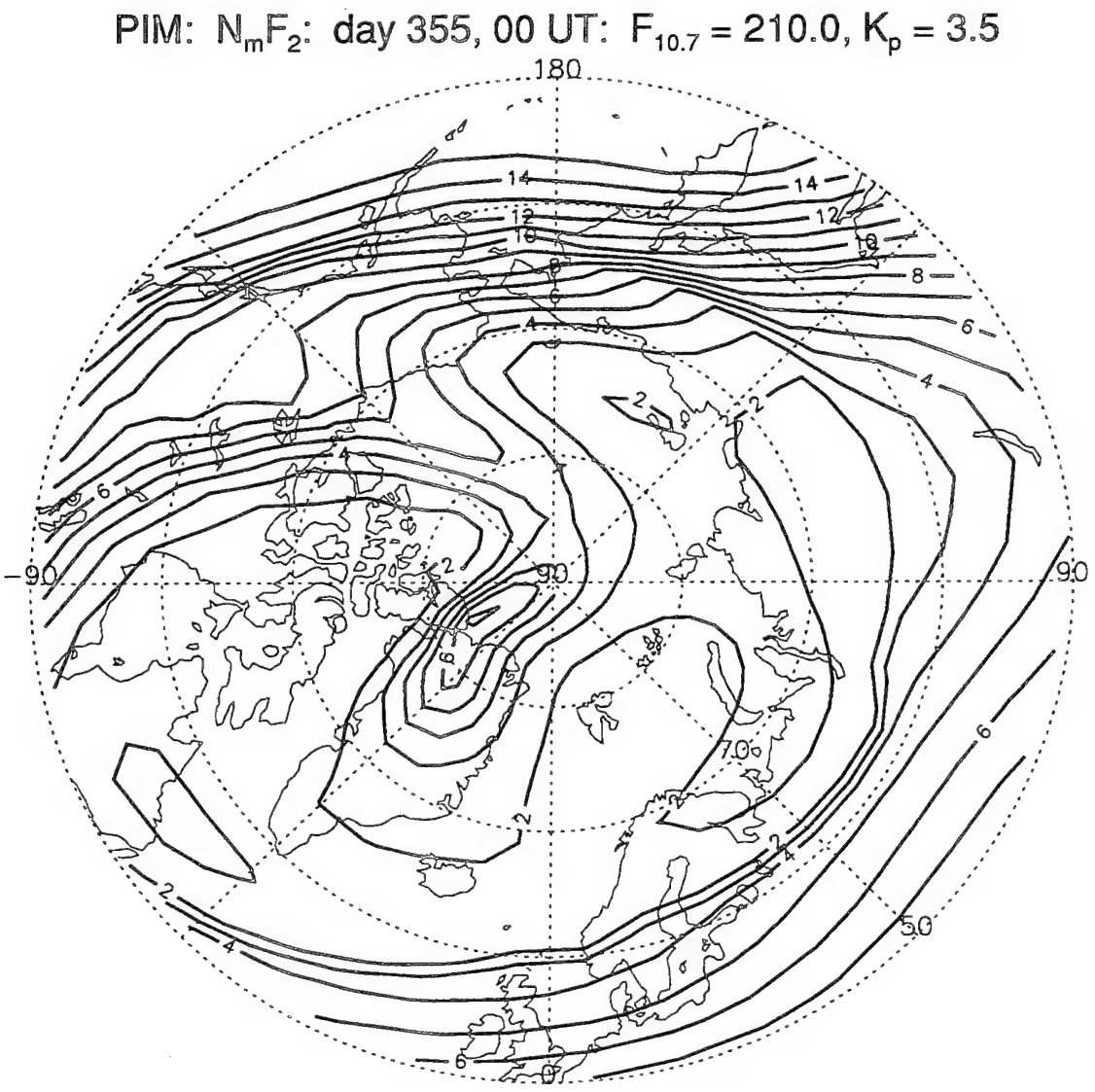

Figure 2. Contours of N_mF_2 (in units of 10^5 cm^{-3}) in polar projection from PIM for the same conditions as Figure 2 except for 00 UT and December solstice. The "tongue of ionization" produced by a steady convection pattern is clearly evident. Local midnight is at the bottom.

4. REAL TIME ADJUSTMENT ALGORITHM

The Real Time Adjustment (RTA) algorithm for the low and middle latitude regions is different from the algorithm used in the high latitude region. This is partly due to the relatively complex morphology of the high latitude ionosphere and partly due to an evolution in our ideas about the real time adjustment process during the development of PRISM.

4.1 Available Data

The near real time data available for use in the adjustment process comes from the Digital Ionospheric Sounding System (DISS), the Ionospheric Monitoring System (IMS), and a suite of Special Sensors on the DMSP satellites. The DISS network consists of a network of digital ionosondes measuring critical frequencies, critical heights, and bottomside profiles. There are projected to be 19 DISS sites when the network is complete. The Ionospheric Monitoring System consists of a separate network of dual frequency GPS receivers measuring TEC. The number is IMS sites is not finallized but is expected to be about five. The DMSP Special Sensors include the in situ plasma properties measured by the SSIES instrument and the precipitating particle measurements of the SSJ/4 instrument. In the future, the SSJ/4 instrument will be replaced by the SSJ/5 instrument and a new set of ionospheric remote sensing instruments, SSUSI and SSULI will be added. SSUSI (a multispectral UV imager) and SSULI (a multispectral limb imager) will make measurements of dayglow, nightglow, and auroral optical emissions (mostly ultraviolet). The observed intensities will be processed on the ground to deduce ionospheric properties in the form of PRISM profile parameters [e.g., *Fox et al.*, 1994]. The two UV imagers will be flown on DMSP beginning some time near the end of the decade.

Because TEC is an integral quantity, it is not easy to incorporate it into the PRISM real time scheme. For PRISM 1.5, we have chosen to convert TEC into an equivalent point datum. Our method for doing so is described in Appendix C.

4.2 *Low and Midlatitude Adjustment Parameters*

The PRISM real time adjustment algorithm operates on six parameters that prescribe how an electron density profile is to be modified or "corrected":

1. $\Delta f_o F_2$, the correction to the model $f_o F_2$,

2. $\Delta f_o E$, the correction to the model $f_o E$,

3. $\Delta h_m F_2$, the correction to the model $h_m F_2$,

4. $\Delta h_m E$, the correction to the model $h_m E$,

5. ΔN_{top}, the correction to the O^+ density at a specific altitude (i.e., the DMSP altitude)

6. ΔH_{top}, the correction to the O^+ scale height at a specific altitude (i.e., the DMSP altitude)

The nominal value for each of these parameters is zero. A positive (negative) value means that the model value must be increased (decreased). Using the available near real time data, the real time adjustment process will assign non-zero values at each location where data is available (the driver sites).

Parameters 1-4 are based on direct measurements by DISS digital ionosondes. Parameter 5 is based on the direct measurement of the O^+ density by the SSIES instrument on board the DMSP satellite. In contrast, Parameter 6 must be inferred from the electron and ion temperatures (T_e, T_i) measured by the SSIES instrument. At midlatitudes, PRISM assumes that the topside ionosphere is in diffusive equilibrium and calculates the topside scale height from

$$H_{top} = \frac{k(T_e + T_i)}{m_{O^+} g} \tag{5}$$

The corresponding model value is obtained from the model O^+ densities (n_2, n_1) at the grid altitudes (z_2, z_1) immediately above and below the DMSP altitude:

$$H_m = \frac{z_2 - z_1}{\ln(n_1/n_2)} \tag{6}$$

At low latitudes, the topside scale height is determined by diffusive processes alone, so the scale height cannot be inferred from the SSIES temperature data.

4.3 *Real Time Adjustment of the Low and Midlatitude Profile Parameters*

In PRISM 1.5, after the values of the profile adjustment parameters have been determined at each driver site, the global correction field is determined using a weighted average method.

1. Given N driver locations and the associated geomagnetic coordinates (λ_n, ϕ_n), let the unadjusted PRISM value at the n^{th} point be u_n and the measured value be v_n.
2. The correction to be applied to the unadjusted PRISM (i.e., PIM) value at the n^{th} point is $c_n = v_n - u_n$.
3. At any other point, (λ, ϕ), the correction to be applied to the PIM value is

$$c(\lambda,\phi) = \frac{\sum_{n=1}^{N} w_n(\lambda,\phi) c_n}{\sum_{n=1}^{N} w_n(\lambda,\phi)} \tag{7}$$

where the $w_n(\lambda,\phi)$ are weight functions that depend on the *distance measure* $d_n(\lambda,\phi)$ between the point (λ,ϕ) and the n^{th} point(λ_n,ϕ_n).

$$w_n(\lambda,\phi) = \frac{\prod_{k=1}^{N} d_k(\lambda,\phi)}{d_n(\lambda,\phi)} = \prod_{k\neq n}^{N} d_k(\lambda,\phi) \tag{8}$$

In PRISM 1.5 we have used the following distance measure.

$$d_n(\lambda,\phi) = \tfrac{1}{2}\left[1 - \cos\gamma_n(\lambda,\phi)\right] \tag{9}$$

where $\gamma_n(\lambda,\phi)$ is the great circle distance between (λ,ϕ) and (λ_n,ϕ_n):

$$\cos\gamma_n(\lambda,\phi) = \sin\lambda \sin\lambda_n + \cos\lambda \cos\lambda_n \cos(\phi - \phi_n) \tag{10}$$

As a practical matter, the actual weighting function used in PRISM is $w_n(\lambda,\varphi) = 1/d_n(\lambda,\varphi)$ unless $d_m(\lambda,\varphi) < \delta$ for some driver station m. In that case, $w_m = 1$ and $w_n = 0$ for $n \neq m$. In PRISM 1.5, δ is set to 10^{-6}.

This method ensures that PRISM will reproduce the input data. However, because the decorrelation length of the ionosphere is of the order of 1000 km or less, no interpolation scheme can hope to accurately reproduce ionospheric parameters where there is no data. Clearly, the denser the data net, the better the model will do. Unfortunately, at least initially, the data will be quite sparse. In order to ensure that sparse datasets do not produce unreasonable ionospheric specifications, PRISM 1.5 checks the spatial distribution of the data and inserts "phantom stations" with the corrections forced to zero. The procedure for placing phantom stations is as follows.

The low and midlatitude region is divided into 32 rectangular subregions with boundaries defined by the following parallels of latitude and meridians of longitude:

parallels of latitude: 60°S, 30°S, 0°, 30°N, and 60°N

meridians of longitude: 30°E, 75°E, 120°E, 165°E, 210°E, 255°E, 300°E, and 345°E

There is a phantom station located at the center of each rectangle. During the data ingestion process, PRISM keeps track of how many stations are located in each rectangular subregion, and how many have f_oF_2 data. As long as at least one station in a subregion reports a value for f_oF_2, then the phantom station for that subregion is ignored. If, however, no station in the subregion reports a value for f_oF_2, then the phantom station is assigned a value equal to the PIM value at that point. A similar procedure is followed for h_mF_2, F_oE, and h_mE data. These phantom stations force the correction field to relax to values near zero in regions where there is no data.

4.4 *Modifying the Low and Midlatitude Model Profiles*

The interpolation method described above provides a global correction field that can be used to calculate the profile correction parameters at any location. In this section, we describe the

way in which the profiles are adjusted using the profile correction parameters. First the layer heights are adjusted, then the layer peak densities, and finally the topside correction is applied.

The layer height correction, using parameters 3 and 4 is a simple shifting of the profiles. If the F layer correction is $\Delta h_m F_2$, then the O^+ profile is shifted so that

$$n_{O^+}{}^{new}(z) = n_{O^+}{}^{old}(z - \Delta h_m F_2) \tag{11}$$

A similar shift is applied to the molecular ion profiles, except that the altitude shift is $\Delta h_m E$.

Once the altitude corrections have been applied, parameters 1 and 2, the critical frequencies, will be used to scale the ion density profiles. For the *F* layer (O^+), the unadjusted peak density is converted to a critical frequency. The correction to be applied (determined by the algorithm in section 4.3) is simply added to the unadjusted frequency. The corrected frequency is then converted back to a density. The ratio of the corrected density to the unadjusted density is used to scale the profile above the peak. Below the peak, an additive correction is applied. This additive correction smoothly vanishes as the altitude approaches $h_m E$. This ensures that F layer corrections do not impact the E layer. This additive correction is described in Appendix C. A similar scaling is applied to the molecular ions except that the additive correction is used above the peak and smoothly vanishes as the altitude approaches $h_m F_2$. This ensures that the E layer corrections do not impact the F layer.

Parameters 5 and 6 are used to correct the topside profile based on n_e, n_i, T_e, and T_i measurements from SSIES on DMSP (nominally 840 km). Let $N_m(z)$ be the model O^+ profile (*after* $f_o F_2$ and $h_m F_2$ corrections have been applied). Further, let $z_p = h_m F_2$, and let z_{top} = the altitude at which ΔN_{top} and ΔH_{top} were measured (usually the DMSP altitude). Let $N_c(z)$ be the corrected profile based on ΔN_{top} and ΔH_{top}. $N_c(z)$ must satisfy the following conditions:

$$N_c(z_{top}) = N_{top} \equiv N_m(z_{top}) + \Delta N_{top} \tag{12}$$

and

$$\frac{1}{H_c(z_{top})} \equiv -\left(\frac{1}{N_c}\frac{\partial N_c}{\partial z}\right)_{z=z_{top}} = \frac{1}{H_{top}} \equiv \frac{1}{H_m(z_{top}) + \Delta H_{top}} \tag{13}$$

In PRISM the corrected profile is obtained from the model profile by scaling the altitude so that

$$N_c(z) = N_m(\zeta) \tag{14}$$

where

$$\zeta(z) = \begin{cases} z, & z \le z_p \\ z_p + \left[2\dfrac{z_1 - z_p}{z_{top} - z_p} - \dfrac{H_m(z_1)}{H_{top}} \right](z - z_p) + \left[\dfrac{H_m(z_1)}{H_{top}} - \dfrac{z_1 - z_p}{z_{top} - z_p} \right] \dfrac{(z - z_p)^2}{z_{top} - z_p}, & z > z_p \end{cases} \tag{15}$$

$$N_m(z_1) = N_{top} \tag{16}$$

and

$$\frac{1}{H_m(z_1)} = -\left(\frac{1}{N_m} \frac{\partial N_m}{\partial z} \right)_{z=z_1} \tag{17}$$

Direct substitution of $z = z_{top}$ in Equation (15) verifies that $\zeta(z_{top}) = z_1$ so that Equation (12) is satisfied. That Equation (13) is satisfied may be seen from

$$\begin{aligned} \frac{1}{H_c(z_{top})} &= -\left(\frac{1}{N_c} \frac{\partial N_c}{\partial z} \right)_{z_{top}} \\ &= -\left(\frac{1}{N_m(\zeta)} \frac{\partial N_m}{\partial \zeta} \frac{\partial \zeta}{\partial z} \right)_{z_{top}} = \frac{1}{H_m(z_1)} \left\{ 2\frac{z_1 - z_p}{z_{top} - z_p} - \frac{H_m(z_1)}{H_{top}} + 2\left[\frac{H_m(z_1)}{H_{top}} - \frac{z_1 - z_p}{z_{top} - z_p} \right] \right\} \\ &= \frac{1}{H_{top}} \end{aligned} \tag{18}$$

This form ensures that the correction and its first derivative vanish at the peak and that the O^+ concentration and its slope are as specified at z_{top}.

When there is no topside scale height data (as at low latitudes), PRISM sets H_{top} to the value

$$H_{top} = \frac{z_1 - z_p}{z_{top} - z_p} H_m \qquad \text{(when } H_{top} \text{ is not determined from data)} \tag{19}$$

so that the altitude scaling becomes linear

$$\zeta(z) = z_p + \frac{z_1 - z_p}{z_{top} - z_p}(z - z_p) \quad \text{(when } H_{top} \text{ is not determined from data)} \qquad (20)$$

An example of the midlatitude profile correction algorithm applied to a single profile is shown in Figure 3, for which we have used Incoherent Scatter Radar (ISR) data from Arecibo to simulate simultaneous digisonde and SSIES data. In this case, the data is from 1800 UT on 4 October 1989. In Figure 3a, the ISR data is compared with the climatology of PIM (i.e., unadjusted PRISM). A profile from the Ionospheric Conductivity and Electron Density (ICED) model [*Tascione et al.*, 1988], which is currently operational at AFSFC is also shown. The actual N_mF_2 is a factor of two higher, and the actual h_mF_2 is about 40 km higher, than the climatological values. In Figure 3b, the PRISM profile has been adjusted only to match the actual N_mF_2. In Figure 3c, both N_mF_2 and h_mF_2 have been adjusted to match the actual data. Finally, in Figure 3d, both the peak and topside adjustments have been made. If we define an RMS density error as

$$\text{RMS density error} = \sqrt{\frac{1}{13}\sum_{k=1}^{13}\left[\frac{N_{PRISM}(z_k) - N_{data}(z_k)}{N_{data}(z_k)}\right]^2} \qquad (21)$$

then PRISM's RMS density error declines from 46% with no profile adjustment to 25% with an N_mF_2 adjustment only, to 18% with both N_mF_2 and h_mF_2 adjusted, and to 16% with both peak and topside adjustments.

Note that in operational use there are normally many data sites, and the topside and bottomside data are seldom colocated. Operationally, PRISM uses all available h_mF_2 and h_mE data to establish global layer height correction fields, then it uses the available N_mF_2 and N_mE data to calculate global profile scaling fields, and finally it uses the topside data to calculate global topside correction fields. These correction fields are then applied to each profile on the output grid as described above.

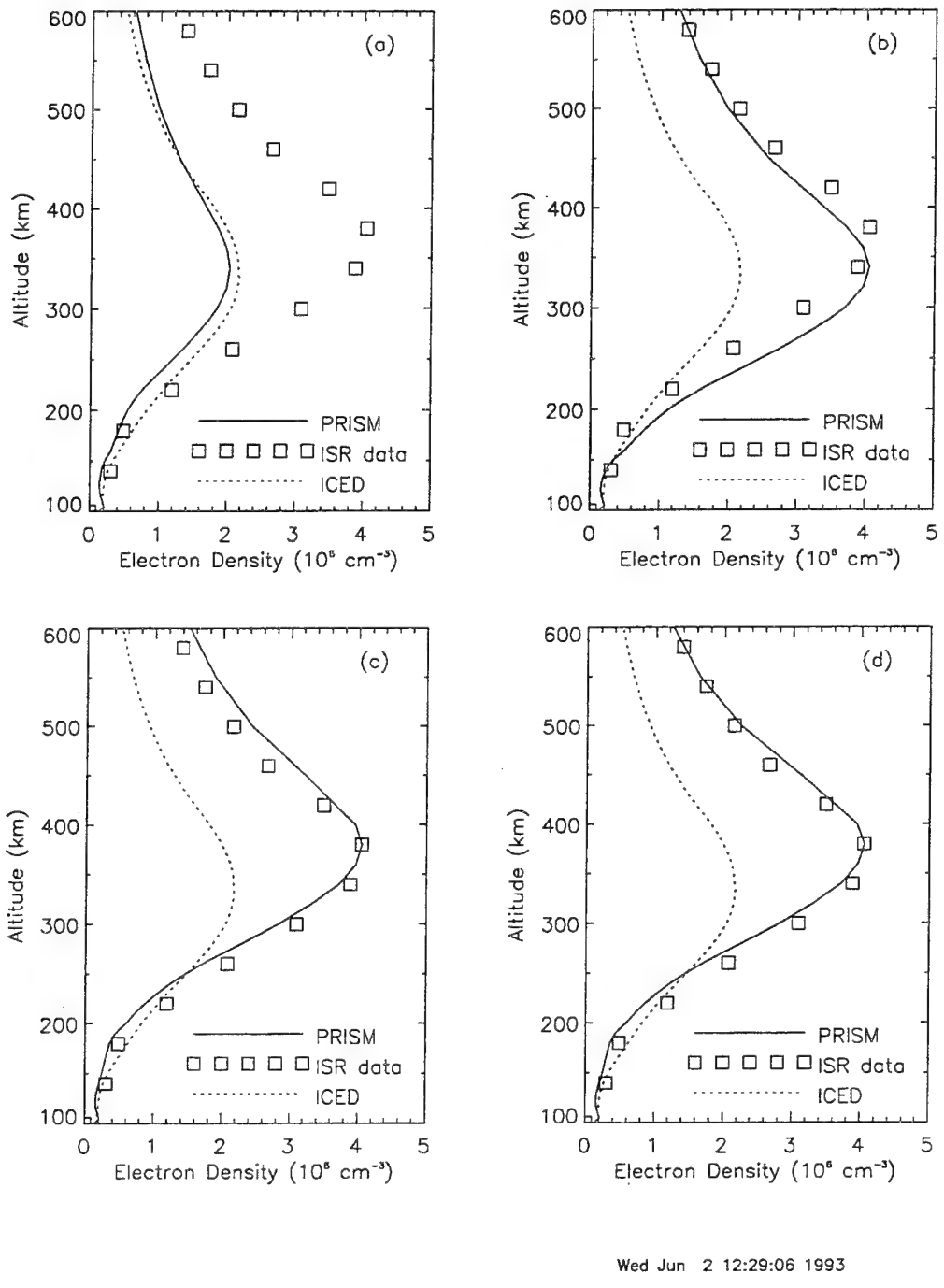

Figure 3. The PRISM profile adjustment procedure illustrated using Incoherent Scatter Radar (ISR) data from Arecibo. (a) No adjustment (i.e., PIM profile): The RMS density error is 46%. (b) N_mF_2 adjustment only: The RMS density error is 25%. (c) N_mF_2 and h_mF_2 adjustment: The RMS density error is 18%. (d) N_mF_2, h_mF_2, and topside adjustments: The RMS density error is 16%.

4.5 *The High Latitude Adjustment Algorithm*

Due to the complexity of the high latitude ionosphere, the real time adjustment algorithm differs appreciably from the low and midlatitude algorithm. Until SSUSI data becomes available, there will be insufficient data to adjust the parameterized USU model in the way that the parameterized low and midlatitude models can be adjusted. Even with SSUSI data, it is not clear that the midlatitude algorithm is appropriate for the high latitude regions.

In PRISM 1.2, the first step in the high latitude real time adjustment process is the establishment of boundary locations. Three boundaries are required: (1) the equatorward edge of the trough, (2) the equatorward edge of the auroral oval, and (3) the poleward edge of the auroral oval.

The equatorward edge of the trough is determined from SSIES drift meter data as the point where the measured ion drift speed departs from the corotation value. The trough boundary as a function of magnetic longitude is given by the formula

$$\theta_t(\varphi) = \theta_0(I_t) + a\exp\left[-\left(\frac{\varphi - b}{c}\right)^p\right]$$

where φ is the magnetic local time (MLT, hours), and I_t is a "trough index" correlated with K_p. $\theta_0(I_t)$ is the radius of the trough boundary at magnetic local midnight and is given by

$$\theta_0(I_t) = 24.4^\circ + 2.12^\circ I_t$$

The second term represents the dayside distortion of the boundary, which would otherwise be a circle centered on the magnetic pole. The parameter values are

a = -10.5°

b = 11.5 hr

c = 3.88 hr

p = 2.73

This model is an approximation to the convection boundaries shown in *Heppner and Maynard* [1987].

The trough index, I_t, is determined according to the following algorithm.

1. If there is no ion drift data, or if a boundary cannot be identified in the data, then $I_t = K_p$.
2. If a single boundary crossing is identified at colatitude θ_b and local time φ_b, then

$$\theta_0 = \theta_b - a \exp\left[-\left(\frac{\varphi_b - b}{c}\right)^2\right]$$

and

$$I_t = \frac{\theta_0 - 24.4^\circ}{2.12^\circ}$$

3. If two or more crossings are identified, then the value of I_t used is the average of the values determined for each crossing.

The boundaries of the auroral oval are determined from electron and ion precipitation data from the SSJ/4 instrument. Separate boundaries are determined for electron and ion precipitation. The algorithm for determining the electron and ion precipitation boundaries from the SSJ/4 data is described in Appendix D.

The next step in the high latitude adjustment process depends on the amount and kind of data available. The decision of how to proceed is made separately for the E layer (NO^+ and O_2^+) and the F layer (O^+). In each case, two choices are available:

F layer:

1. Perform a simple least squares adjustment of the USU O^+ model.
2. Use a semi-empirical f_oF_2 model (FMODEL) to adjust the USU O^+ profiles.

E layer:

1. Perform a simple least squares adjustment of the USU NO^+ and O_2^+ models.
2. Use a fast, first principles, E layer local chemistry model (HLE).

The decision matrix used in PRISM is shown in Table5.

Table 5. PRISM High Latitude Decision Matrix

Data Available?			Model Used by PRISM	
DISS	SSIES	SSJ/4	*F* layer	*E* layer
Yes	Yes	Yes	FMODEL	HLE
Yes	Yes	No	FMODEL	USU
Yes	No	Yes	FMODEL	HLE
Yes	No	No	USU	USU
No	Yes	Yes	USU	USU
No	Yes	No	USU	USU
No	No	Yes	USU	USU
No	No	No	USU	USU

In experimenting with high latitude data, we found that extrapolating SSJ/4 data taken along the DMSP orbital track to points well away from the orbital track was very risky. We found no suitable model of the *instantaneous* auroral precipitation for this extrapolation. When SSUSI auroral image data becomes available, this limitation will be removed because much less extrapolation will be required. It should be possible to use HLE whenever timely SSUSI images are available.

FMODEL is a semi-empirical model of f_oF_2 based on a combination of theory and data. It is divided into three regions: the subauroral trough, the auroral oval, and the polar cap. The f_oF_2 determined by least squares adjustment of the model parameters is used to scale the USU O^+ profiles. No further adjustment of the profiles is performed.

The subauroral trough is divided into two local time regimes: evening (from 1200 to 0000 MLT) and morning (from 0000 to 1200 MLT). Each trough (morning and evening) has a depth

parameter that specifies the difference between the midlatitude value of f_oF_2 at the equatorward edge and the trough minimum. The local time variation of the trough depth is fixed (not part of the least squares adjustment process). If the width of the trough is less than 3°, the depth is reduced in proportion to the width so that when the width vanishes so does the depth. The thickness of the (equatorward) trough wall is always 60% of the total width of the trough. The poleward edge of the trough is the equatorward edge of the auroral F-layer, so the poleward "wall" is considered to be part of the auroral region.

At fixed magnetic local time, the auroral F layer f_oF_2 is simply a cubic polynomial in magnetic latitude:

$$f_oF_2(\lambda) = f_{max} + A(\lambda - \lambda_{max})^2 + B(\lambda - \lambda_{max})^3$$

where $f_{max} = f_oF_2(\lambda_{max})$ is an extremum, and A and B are chosen so that f_oF_2 is continuous across the boundaries with the trough and polar cap.

The background polar cap f_oF_2 is obtained from the URSI coefficients using an internally derived effective sunspot number, the value of which is determined as part of the least squares adjustment process based on ionosonde data. It should be noted that this part of the model describes only the background polar cap ionosphere, not "polar cap patches" or "polar cap arcs."

5. VALIDATION

Prior to delivery to the Air Force Space Forecast Center, and earlier version of PRISM (1.2) underwent an extensive validation using historical data approximating the kinds of data that will be available to PRISM in operational use. The results of this validation effort were reported in *Daniell et al.* [1994] and are not repeated here. Since PRISM 1.5 incorporates several substantial changes from PRISM 1.2, a new validation will be carried out in the future under a separate contract.

6. DISCUSSION

We have described the development of PRISM, a real time ionospheric specification model based on parameterized theoretical ionospheric models. Unlike previous specification models, PRISM is based on physical models rather than empirical models. PRISM consists of two parts: the parameterized physical models (PIM) and a real time update system that ingests both ground-based and space-based data and modifies PIM profiles accordingly. PRISM provides considerable improvement over simple climatology in the vicinity of the data sources and does no worse than climatology at locations remote from the data. With the advent of remote ionospheric sensing using UV airglow and auroral emissions measured from satellites and the proliferation of dual frequency GPS receivers providing line of sight TEC measurements, we expect this approach to provide improved ionospheric specifications in near real time for the AFSFC and its customers.

A number of compromises were required in the development of PIM and PRISM. First, of course, was the necessity of using parameterizations (in the form of diurnally reproducible runs) of the physical models, rather than the physical models themselves. Second, we had to use empirical models (e.g., MSIS-86) instead of physical models to provide the necessary inputs to the ionospheric models. Third, we had to use a tilted dipole representation of the earth's magnetic field instead of a more realistic model. This last compromise is mitigated somewhat by the use of Corrected Geomagnetic (CGM) coordinates in PIM and PRISM. While not fully self-consistent, this does allow a more realistic representation of geomagnetically controlled features such as the equatorial anomaly. We expect to remove the compromises as available computing power increases in the future.

The particular features described here apply to PRISM version 1.5 and PIM version 1.3. Significant enhancements to both PIM and PRISM are planned for the near future. H^+ ion densities based on a parameterization of the plasmasphere model of *Bailey and Sellek* [1990] will be added so that PIM and PRISM can give electron density profiles up to the plasmapause. At the same time the coefficient files will be regenerated using a single global ionospheric model, eliminating the need to merge models across region boundaries. The parameterization process

will also be reexamined in order to produce a more accurate and more efficient analytic fit to the model runs. The resulting version of PRISM, while considerably enhanced, will be designed to fit into AFSFC's operational configuration with no changes to the existing software that interacts with PRISM 1.5.

Appendix A. Empirical Orthonormal Functions

This treatment of empirical orthogonal functions (EOF's) is based on the Appendix of *Secan and Tascione* [1984], which was based on *Lorenz* [1956], *Kutzbach* [1967], and *Davis* [1976]. See also *Peixota and Oort* [1991]. The reader is referred to these references for mathematical proofs of the assertions made below. In the following discussion, we use the notation given in Table 3 of the main text.

A database consists of altitude profiles at certain longitudes, certain latitudes, and certain Universal Times. (See Tables 1-4 of the main text.) Let S be the number of altitude profiles in a database, and let I be the number of points in each altitude profile. We would like to represent each altitude profile of the quantity Ψ (e.g., O^+ concentration) as an expansion in orthogonal functions, $g_m(z_i)$:

$$\Psi_s(z_i) = \sum_{m=1}^{M} \alpha_{sm} g_m(z_i) + r_s(z_i), \qquad s = 1...S,\ i = 1...I \tag{A1}$$

where $r_s(z_i)$ is the residual, and the coefficients α_{sm} are calculated from

$$\alpha_{sm} = \sum_{i=1}^{I} \Psi_s(z_i) g_m(z_i) \tag{A2}$$

In principle, any orthogonal set of functions may be used. However, the references cited above provide an algorithm for finding the set which minimizes the RMS error for a given number of terms, $M \le I$. We summarize the algorithm here.

First define the $I \times I$ covariance matrix $\mathbb{C}$ with elements

$$C_{ij} = \frac{1}{S} \sum_{s=1}^{S} \Psi_s(z_i) \Psi_s(z_j), \qquad i, j = 1,2,...I \tag{A1}$$

Now consider the eigenvalue/eigenvector problem $\mathbb{C}\varphi = \varphi\mathbb{L}$ or

$$\sum_{j=1}^{I} C_{ij} \varphi_{jk} = \sum_{j=1}^{I} \varphi_{ij} \delta_{jk} \lambda_k = \varphi_{ik} \lambda_k \tag{A2}$$

where $\varphi = \{\varphi_{ij}\}$ is the matrix of eigenvectors of $\mathbb{C} = \{C_{ij}\}$, and $\mathbb{L} = \{\delta_{ij}\lambda_j\}$ is a diagonal matrix whose elements are the corresponding eigenvalues. (The k^{th} column of φ is the eigenvector

corresponding to the k^{th} eigenvalue, λ_k.) By convention, the eigenvectors and eigenvalues are ordered so that $\lambda_1 > \lambda_2 > ... > \lambda_I$. Because **C** is a real symmetric matrix, eigenvectors corresponding to unique eigenvalues are guaranteed to be orthogonal [See, e.g., *Hildebrand*, 1965]. Because of the origin of the matrix **C**, it is unlikely that any of its eigenvalues will be degenerate, so we may assume that φ is an orthogonal set. According to *Secan and Tascione* [1984] and references therein, the set of orthogonal functions that minimizes the RMS error for M terms is just the first M eigenvectors:

$$g_m(z_i) = \varphi_{im}, \qquad i = 1,2,...I;\ m = 1,2,...M \tag{A3}$$

These are the Empirical Orthonormal Functions (EOFs).

As a practical matter, we have found that the number of EOFs needed to provide a reasonably good representation for all the profiles is about $I/6$, as illustrated in Table 4 in the main text. The only exception is the low and midlatitude E layer (NO^+ and O_2^+), probably because these databases covered both hemispheres simultaneously. We have also found that substantial improvement in representation does not occur until the number of EOF's is about $I/2$. Furthermore, the EOF's derived for one database were inadequate for any other database, and the EOF's simultaneously derived from several databases produce noticeably poorer representations than those derived for each database individually. Consequently, we have derived separate EOF sets for each database.

The first nine EOF's derived from the low latitude F region (O^+) database for the US longitude sector, the December solstice, and moderate solar activity, are shown in Figure A1. The first EOF always has the least structure, and successive EOF's become progressively more structured. Although differing in detail, the EOF's for the other databases are qualitatively similar.

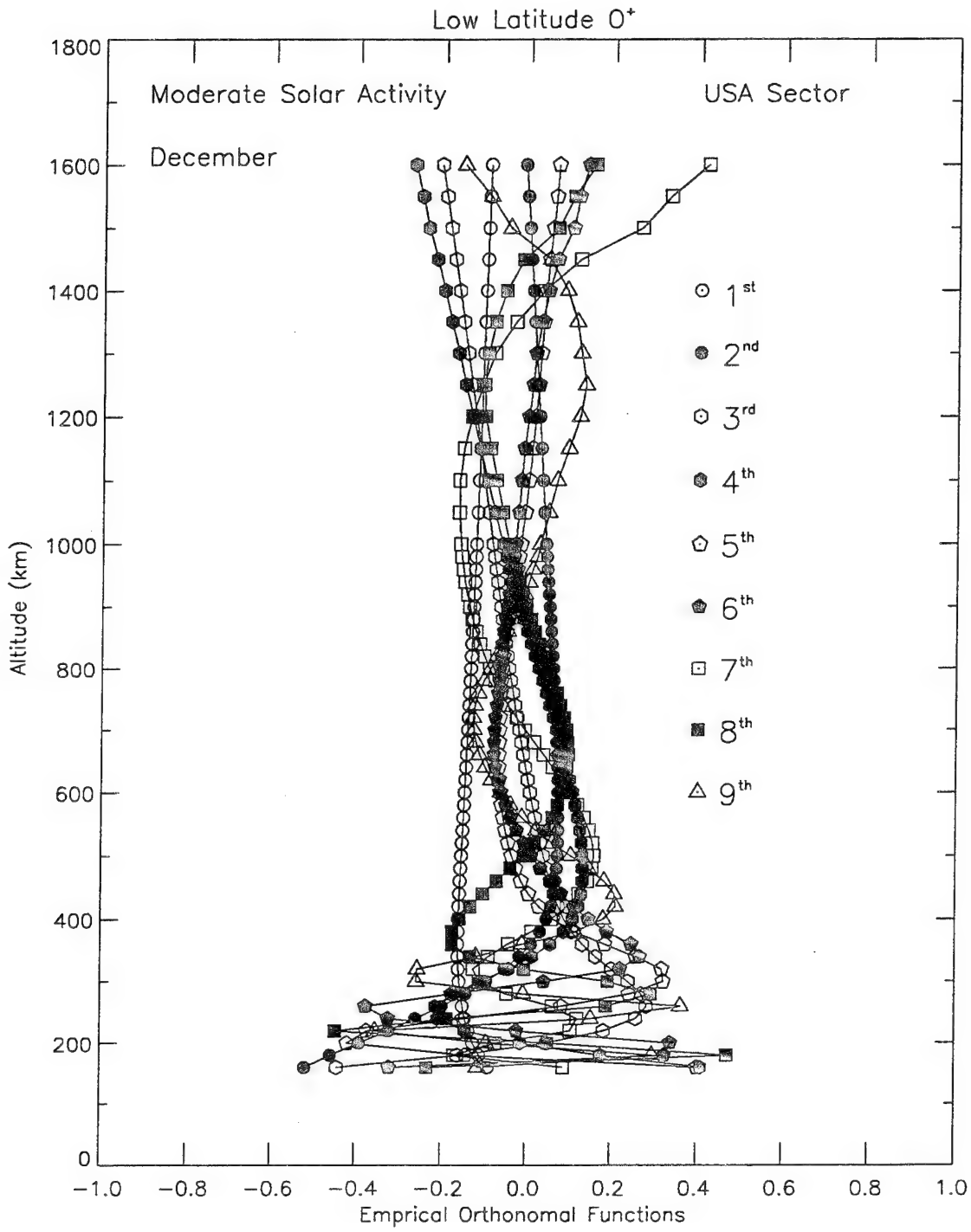

Figure A1. The Empirical Orthonormal Functions (EOF's) for low latitude O^+ derived from the LOWLAT output databases for the USA longitude sector, December solstice, moderate magnetic activity, and moderate solar activity. Only the first nine EOF's are plotted because these are the ones used in PIM and PRISM.

Appendix B. Orthogonal Polynomials of Discrete Variables

Because the databases to which we desire analytic approximations have discrete latitude grids, we preferred to use polynomials whose orthogonality is defined in terms of that grid, rather than in terms of integrals over the interval. The algorithm for generating orthogonal polynomials on a specified grid is given by *Beckmann* [1973]. Let us denote the desired polynomials by $u_n(\lambda)$ and define $u_{-1}(\lambda) \equiv 0$ and $u_0(\lambda) \equiv 1$. Note that the polynomials are continuous functions of the continuous variable λ even though their orthogonality is defined in terms of the discrete grid $\{\lambda_j, j = 1,2,\ldots J\}$. The recursion relation for the polynomials is

$$u_{n+1}(\lambda) = (\lambda - B_n)u_n(\lambda) - \frac{h_n^2}{h_{n-1}^2}u_{n-1}(\lambda) \tag{B1}$$

where the norms h_n are given by

$$h_n = \sum_{j=1}^{J} u_n^2(\lambda_j) \tag{B2}$$

and the recursion constants B_n are given by

$$B_n = \frac{1}{h_n^2}\sum_{j=1}^{J} \lambda_j u_n(\lambda_j) \tag{B3}$$

The polynomials generated by this algorithm may be used to represent the latitude variations of the Fourier coefficients a_{mp} and b_{mp} (see main text):

$$a_{mp}(\lambda_j, \tau_l) = \sum_{n=1}^{N} \alpha_{mnp}(\tau_l) u_n(\lambda_j) \tag{B4}$$

$$b_{mp}(\lambda_j, \tau_l) = \sum_{n=1}^{N} \beta_{mnp}(\tau_l) u_n(\lambda_j) \tag{B5}$$

where

$$\beta_{mnp}(\tau_l) = \frac{1}{h_n^2}\sum_{j=1}^{J} a_{mp}(\lambda_j, \tau_l) u_n(\lambda_j) \tag{B6}$$

$$\beta_{mnp}(\tau_l) = \frac{1}{h_n^2}\sum_{j=1}^{J} b_{mp}(\lambda_j, \tau_l) u_n(\lambda_j) \tag{B7}$$

Appendix C. *F*-layer Density Scaling Algorithm and TEC Adjustments

In order to be able to adjust *E*- and *F*-layer parameters separately, PRISM uses an altitude dependent scaling algorithm for each layer. Because the TEC adjustment process is dependent on the details of the *F*-layer adjustment process, they are described together.

For altitudes above h_mF_2 the adjustment is a simple multiplicative scaling:

$$n_{O^+}^{(new)}(z) = S_F n_{O^+}^{(old)}, \qquad z \geq h_mF_2 \tag{C1}$$

where

$$S_F = \frac{N_mF_2^{(new)}}{N_mF_2^{(old)}} \tag{C2}$$

When $N_mF_2^{(new)}$ is derived from DISS or other ionosonde data, it is simply

$$N_mF_2^{(new)} = 1.24\times10^4\left(f_oF_2^{(\mathrm{DISS})}\right)^2 \tag{C3}$$

where $f_oF_2^{(\mathrm{DISS})}$ is the measured value in MHz and $N_mF_2^{(new)}$ is in cm^{-3}.

For altitudes below h_mF_2, the adjustment is additive and vanishes gradually as z approaches h_mE.

$$n_{O^+}^{(\mathrm{new})}(z) = n_{O^+}^{(\mathrm{old})}(z) + \Delta n_{O^+}(z) \tag{C4}$$

where

$$\Delta n_{O^+}(z) = \begin{cases} \left(N_mF_2^{(new)} - N_mF_2^{(old)}\right)\dfrac{\exp\left(\dfrac{z-h_mF_2}{W}\right) - \exp\left(\dfrac{h_mE-h_mF_2}{W}\right)}{1-\exp\left(\dfrac{h_mE-h_mF_2}{W}\right)}, & h_mE < z < h_mF_2 \\ 0, & z \leq h_mE \end{cases} \tag{C5}$$

The value of the parameter W is determined by the shape of the bottomside O^+ density profile, and is usually of the order of 100 km.

In order to use TEC data, PRISM must convert the TEC measurement into an equivalent point measurement. TEC data is ingested as vertical equivalent TEC at the Ionospheric Intersection Point (IIP). If the IIP is farther than 1000 km from the nearest DISS site, then the TEC is converted into an equivalent N_mF_2. PRISM converts the observed vertical equivalent TEC (TEC_{obs}) into an F-layer correction factor that is applied in the same way as the correction factors derived from DISS (ionosonde) data. First, PRISM calculates a TEC correction as

$$\Delta TEC = TEC_{obs} - TEC_{PRISM} \tag{C6}$$

The equivalent N_mF_2 correction is determined from

$$\Delta TEC = \int_0^\infty \left[n_{O^+}^{(new)}(z) - n_{O^+}^{(old)}(z) \right] dz \tag{C7}$$

or

$$\Delta TEC = W_b \Delta N_m F_2 + S_F \int_{h_mF_2}^\infty n_{O^+}^{(old)}(z)\, dz \tag{C8}$$

where

$$W_b = W - \frac{(h_mF_2 - h_mE)}{\exp\left(\frac{h_mF_2 - h_mE}{W}\right) - 1} \tag{C9}$$

Therefore, the value of $N_mF_2^{(new)}$ corresponding to TEC_{obs} is

$$N_mF_2^{(new)} = \frac{TEC_{obs} - TEC_{PRISM} - W_b N_m F_2^{(old)}}{W_b N_m F_2^{(old)} + \int_{h_mF_2}^\infty n_{O^+}^{(old)} dz} N_mF_2^{(old)} \tag{C10}$$

From this point, PRISM treats TEC data as if it were ionosonde data with h_mF_2 missing.

If the IIP is within 1000 km of a DISS site, then the TEC measurement is converted into an equivalent SSIES density measurement. First, the $\Delta f_o F_2$ and $\Delta h_m F_2$ corrections determined from the nearest DISS site is applied to the PIM profile at the IIP. Then the topside portion of the profile is corrected to force agreement with the TEC measurement:

$$n_{O^+}^{(new)}(z) = n_{O^+}^{(old)}(\zeta) \tag{C11}$$

$$\zeta(z) = \begin{cases} z, & z \le h_m F_2 \\ h_m F_2 + a(z - h_m F_2), & z > h_m F_2 \end{cases} \tag{C12}$$

where a is a scale factor to be determined from TEC.

The difference in TEC, as defined by Equation 6), is

$$\Delta\text{TEC} = \int_{h_m F_2}^{\infty} n_{O^+}^{(new)} dz - \int_{h_m F_2}^{\infty} n_{O^+}^{(old)} dz \tag{C13}$$

or

$$\Delta\text{TEC} = \frac{1-a}{a} \int_{h_m F_2}^{\infty} n_{O^+}^{(old)} dz \tag{C14}$$

resulting in

$$a = \frac{\int_{h_m F_2}^{\infty} n_{O^+}^{(old)} dz}{\Delta\text{TEC} + \int_{h_m F_2}^{\infty} n_{O^+}^{(old)} dz} \tag{C15}$$

If we identify the scale factor a with the ratio $(z_1 - h_m F_2)/(z_d - h_m F_2)$, then

$$z_1 = h_m F_2 + (z_d - h_m F_2) a \tag{C16}$$

$$N_{top} = n_{O^+}^{(old)}(z_1) \tag{C17}$$

and

$$H_{top} = aH_m \tag{C18}$$

If the IIP is within 1000 km of both a DISS station and a DMSP orbital track, the TEC measurement is ignored. In a future version of PRISM, in which the plasmasphere is included, TEC measurements in such situations will be used to constrain the H^+ density.

Appendix D. Auroral boundary determination

There are four auroral precipitation boundaries in each hemisphere: The equatorward and poleward electron boundaries and the equatorward and poleward ion boundaries. Since there are always two DMSP satellites in orbit, there are potentially four crossings of each boundary. The specification of a given boundary depends on the number of crossings detected in the data. The boundary detection is performed as follows.

1. If SSJ/4 data are available, then divide each orbit's worth of data into four segments, each segment extending from the most equatorward point to the most poleward point.
2. Each segment is searched from equator toward the pole until the electron energy flux exceeds 0.25 erg cm^{-2} s^{-1} (for the equatorward electron boundary) and the ion energy flux exceeds 0.1 erg cm^{-2} s^{-1} (for the equatorward ion boundary).
3. Search each segment from pole toward the equator until the same thresholds are exceeded to establish the poleward boundaries.

The boundaries are always assumed to be circular. The specification of each boundary circle (in terms of its center and radius) depends on the number of crossings detected.

1. If four crossings are found, there are four possible combinations of three points. Each of the four possible combinations defines a circle, which may be described by its center and radius. The center coordinates and radii of the four circles are averaged to determine the boundary used in PRISM.
5. If only three crossings are found, the boundary is uniquely defined by the circle passing through the three points.
6. If only two crossings are found, the boundary is taken to be the circle that passes through both points and has a radius equal to the mean of the colatitudes of the two points.

If only one crossing of a boundary is found, or if no crossings are found (or SSJ/4 data is missing), the boundaries are determined as follows. Equatorward boundaries are based on an

analytic representation of the *Gussenhoven et al.* [1983] boundary. The boundary itself is a circle whose center is displaced from the magnetic pole. The radius (in degrees) of the circle is

$$\theta_1(P_1) = 20.9° + 1.7° P_1$$

where P_1 is a "precipitation index". The center of the circle is located at

$$\lambda_{c1}(P_1) = 87.3°–0.267° P_1$$

$$\varphi_{c1}(P_1) = 39.5°–1.25° P_1 + 0.076° P_1^2$$

where λ_{c1} is magnetic latitude and φ_{c1} is magnetic local time (in degrees).

Poleward boundaries have almost the same form, except that they are parameterized in terms of a separate "precipitation index" P_2.

$$\theta_2(P_2) = 13.4° + 1.7° P_2$$

$$\lambda_{c2}(P_2) = \begin{cases} 89.2°+0.267° P_2, & P_2 < 3 \\ 90.8°–0.267° P_2, & P_2 \geq 3 \end{cases}$$

$$\varphi_{c2}(P_2) = \begin{cases} \varphi_{c1} + 180°, & P_2 < 3 \\ \varphi_{c1}, & P_2 \geq 3 \end{cases}$$

If there is no data, or if no boundaries are detected in the data, then $P_1 = P_2 = K_p$. However, if a single crossing is detected, then the precipitation index is chosen so that the above boundary matches the crossing.

PRISM 1.4 External Input/Output File Specifications
(i.e. files created by or under the control of the User)

CONTENTS

Input Files

Output Files

PRISM 1.5
30 May 1995

Input Stream Specification for PRISM 1.5
30 May 1995

Record #	Element Name	Data Type	ASCII Format	Units	Description	Repetition Rate	Notes
1	INTER	Character	"N"	N/A	"N" indicates this is a batch run (interactive runs are not supported in PRISM 1.5)	1 per file	
2	YEAR	Integer	XXXX	years	4 digit year (e.g., 1989)	1 per file	
3	DAY	Integer	XXX	days	day of year (1 Jan = 001, etc.)	1 per file	
4	UT	Integer	XXXX	hours and minutes	Universal Time of observation in HHMM format	1 per file	
5	ST_OUT	Integer	X	N/A	Type of output for station sites: 0 = profile parameters (critical frequencies and layer heights) only 1 = electron density profiles only 2 = both profile parameters and electron density profiles 3 = no output at station sites	1 per file	
6	GR_OUT	Integer	X	N/A	Type of output for grid points: 0 = profile parameters only 1 = electron density profiles only 2 = both profile parameters and electron density profiles 3 = no gridded output	1 per file	
7	FNORM	Integer	X	N/A	Normalization for f_oF_2: 0 = normalize to URSI-88 1 = no normalization	1 per file	

Record #	Element Name	Data Type	ASCII Format	Units	Description	Repetition Rate	Notes
8	SSNSRC	Integer	X	N/A	Source indicator for SSN_{eff} : 0 = determine SSN_{eff} from DISS and IMS input, using input value as starting point 1 = use input value of SSN_{eff} (Record 26, SSNEFF)	1 per file	1
9	ST_DIF	Character	"Y" or "N"	N/A	"Y" if output stations are different than input stations.	1 per file	2
10	ST_FIL	Character	see note 3	N/A	name of file containing list of output stations.	1 per file	3
11	GR_FIL	Character	see note 5	N/A	output file name for gridded output, e.g., "TEST1.OUT"	1 per file	4,5
12	USRGRD	Character	"Y" or "N"	N/A	"Y" indicates that a user specified grid will be used; "N" indicates that the default grid will be used	1 per file	4
13	G_OR_M	Character	"G" or "M"	N/A	gridded output coordinate system: "G" = geographic (geocentric) "M" = corrected geomagnetic	1 per file	4
14	LATSW	Real	±XX.XX	degrees	latitude of southwest corner of user specified grid (positive north)	1 per record	6
	LONSW	Real	±XXX.XX	degrees	longitude of southwest corner of user grid (positive east)	1 per record	
15	LATNE	Real	±XX.XX	degrees	latitude of northeast corner of user specified grid (positive north)	1 per record	6
	LONNE	Real	±XXX.XX	degrees	longitude of northeast corner of user grid (positive east)	1 per record	

Record #	Element Name	Data Type	ASCII Format	Units	Description	Repetition Rate	Notes
16	SPACNG	Character	"N" or "G"	N/A	"N" indicates user will specify number of grid points; "G" indicates user will specify size of grid intervals	1 per file	6
17	NUMLAT	Integer	XXX	N/A	number of latitude points in user specified grid	1 per record	7
	NUMLON	Integer	XXX	N/A	number of longitude points in user specified grid	1 per record	
18	DLAT	Real	±XX.XX	degrees	latitude spacing of user specified grid	1 per record	8
	DLON	Real	±XXX.XX	degrees	longitude spacing of user specified grid	1 per record	
19	USRALT	Character	"Y" or "N"	N/A	"Y" indicates that user will specify output altitude grid; "N" indicates that default altitude grid will be used	1 per file	9
20	ALTFIL	Character	see note 9	N/A	name of file containing user specified altitude grid	1 per file	10
21	RKP	Real	X.X	N/A	K_p value for UT of run	1 per file	
22	BZ	Real	±XX.X	nT	z-component of Interplanetary Magnetic Field (IMF).	1 per record	11
	BY	Real	±XX.X	nT	y-component of IMF	1 per record	
23	F10P7A	Real	XXX.X	solar flux units	90 day mean $F_{10.7}$ value (as used by MSIS model)	1 per file	

Record #	Element Name	Data Type	ASCII Format	Units	Description	Repetition Rate	Notes
24	F10SSN	Integer	X	N/A	specifies relationship between $F_{10.7}$ and effective SSN: 0 = SSN and $F_{10.7}$ are unrelated 1 = SSN is computed from $F_{10.7}$ 2 = $F_{10.7}$ is computed from SSN	1 per file	12
25	F10P7	Real	XXX.X	solar flux units	the daily $F_{10.7}$ value (most recent measurement)	1 per file	
26	SSNEFF	Real	XXX.X	N/A	effective sunspot number	1 per file	13
27	blank line	N/A	N/A	N/A	3 blank lines	3 per file	
28	CHANGE	Character	"N"	N/A	see note 14	1 per file	14
29	blank line	N/A	N/A	N/A	1 blank line	1 per file	

General Notes:

The Data Element Names do not necessarily correspond to the FORTRAN variable names in the source code. This is because the FORTRAN names are not always descriptive of the actual contents of the data element (for historical reasons).

Shaded records indicate that the record's presence is contingent on the contents of one or more preceding records.

Because PRISM uses FORTRAN list directed input for all numeric input, the numeric format is flexible. The formats indicated in the table are suggested formats only. Plus (+) signs are always optional. The variables may be separated by (a) one or more spaces, (b) a comma (,), or (c) a comma and one or more spaces.

Numbered Notes:

1. This record is present only if FNORM (record 7) is 0.
2. This record is present only if ST_OUT (record 5) is 0, 1, or 2.
3. This record is present only if ST_DIF (record 9) is "Y". It should contain a valid file name of or more than 32 characters, and the file must be located in the directory specified in record 3 of the file PATH_NAME.TXT. (See *Data Control Input Specification for PRISM*.)
4. This record is present only if GR_OUT (record 6) is 0, 1, or 2.

5. If present, record 11 must contain a valid file name of no more than 32 characters. The file will be written to the default directory (the one containing PRISM.EXE).
6. This record is present only if USRGRD (record 12) is present and contains "Y".
7. This record is present only if SPACNG (record 16) is present and contains "N".
8. This record is present only if SPACNG (record 16) is present and contains "G".
9. This record is present only if one or both of ST_OUT (record 5) or GR_OUT (record 6) has the value 1 or 2.
10. This record is present only if USRALT (record 19) contains "Y". If present, it must contain a valid file name of no more than 32 characters, and the file must be located in the default directory.
11. nT = nanoTesla. PRISM uses only the sign of B_z and B_y to select coefficients corresponding to Heppner-Maynard convection patterns, so the units are not crucial, and even a crude estimate is useful.
12. F10SSN = 0 is strongly recommended.
13. This record is present only if F10SSN (record 24) contains 0 or 2.
14 CHANGE (record 28) should always contain "N".

Original document:	2 September 1994	
correction 1:	16 September 1994	(record 19 and note 9)
correction 2:	3 November 1994	(record 15)
correction 3:	30 May 1995	(records 1,27-29) Version 1.5

Data Control Input File Specification for PRISM 1.5
30 May 1995

File Name: PATH_NAM.TXT

Record #	Element Name	Data Type	ASCII Format	Units	Description	Repetition Rate	Notes
1	DACCES	Integer	X	N/A	indicates how direct access files are opened. Should always be 2 for VAX VMS systems. See note 1.	1 per file	1
2	CGPATH	Character	see note 2	N/A	specifies the directory that contains the file that contains the coefficients for converting from geocentric to corrected geomagnetic coordinates.	1 per file	2,3
3	RTPATH	Character	see note 2	N/A	specifies the directory containing the real time data (DISS, TISS, SSIES, SSJ/4, etc.)	1 per file	
4	USUPATH	Character	see note 2	N/A	specifies the directory containing the USU model coefficient databases.	1 per file	
5	MFPATH	Character	see note 2	N/A	specifies the directory containing the midlatitude F layer coefficient databases	1 per file	
6	LFPATH	Character	see note 2	N/A	specifies the directory containing the low latitude F layer coefficient databases	1 per file	
7	LMEPATH	Character	see note 2	N/A	specifies the directory containing the low and midlatitude E layer coefficient databases	1 per file	
8	HLEPATH	Character	see note 2	N/A	specifies directory containing files needed by HLE (High Latitude E-layer model).	1 per file	
9	URSIPATH	Character	see note 2	N/A	specifies directory containing the URSI-88 coefficients	1 per file	

Record #	Element Name	Data Type	ASCII Format	Units	Description	Repetition Rate	Notes
10	DISS	Character	see note 4	N/A	identifies file(s) containing DISS data.	5 per record	4
11	DMSP	Character	see note 4	N/A	identifies file(s) containing DMSP (SSIES & SSJ/4) data.	8 per record	4
12	TISS	Character	see note 4	N/A	identifies file(s) containing TISS data.	5 per record	4

General Notes:

The Data Element Names do not necessarily correspond to the FORTRAN variable names in the source code. This is because the FORTRAN names are not always descriptive of the actual contents of the data element (for historical reasons).

Numbered Notes:

1. VAX VMS FORTRAN opens direct access files with record lengths specified in longwords (4 byte words). DOS and UNIX FORTRAN usually open direct access files with record lengths specified in bytes. For the latter case, the value should be specified as 1.
2. Directory (or path) names must be valid directory names of no more than 80 characters in length.
3. The coefficient file is named CGLALO.DAT.
4. This record may contain up to five fields. Each field is exactly 11 characters in length. Each field may contain one file name, left justified, of no more than 10 characters. The 11th character is used for improved readability and is ignored by PRISM. The file names actually represent prefixes to the full file names of the form "xxxxxxxxxx.DAT". The user is free to choose any unique character string (of 10 characters or less) but blank fields are ignored. (That is, PRISM does not attempt to open files named ".DAT".) If there is no data of this type, the record should be empty or blank.

Original Document	2 September 1994	
Revisions	9 January 1995	(Note 4 clarified, Note 5 eliminated)
Version 1.5	30 May 1995	(No changes except version number)

Ionosonde (DISS) Input Files for PRISM 1.5
30 May 1995

Record #	Element Name	Data Type	ASCII Format	Units	Description	Repetition Rate	Notes
1...N	YEAR	Integer	XXXX	years	4 digit year of observation	1 per record	1
	DAY	Integer	XXX	days	day of year of observation	1 per record	
	UT	Integer	XXXX	hours and minutes	Universal Time of observation in HHMM format	1 per record	
	GLAT	Real	±XX.XX	degrees	geographic latitude of ionosonde	1 per record	
	GLON	Real	±XXX.XX	degrees	geographic longitude of ionosonde	1 per record	
	FOF2	Real	XX.XX	MHz	observed critical frequency of the F_2 layer	1 per record	
	HMF2	Real	XXX.X	km	observed height of the F_2 layer	1 per record	
	FOF1	Real	XX.XX	MHz	observed critical frequency of the F_1 layer	1 per record	2
	HMF1	Real	XXX.X	km	observed height of the F_1 layer	1 per record	2
	FOE	Real	XX.XX	MHz	observed critical frequency of the E layer	1 per record	
	HME	Real	XXX.X	km	observed height of the E layer	1 per record	
	OPTIONAL	Character	N/A	N/A	Optional information (e.g., WMO number): ignored by PRISM, may be left blank	1 per record	

General Notes:

The Data Element Names do not necessarily correspond to the FORTRAN variable names in the source code. This is because the FORTRAN names are not always descriptive of the actual contents of the data element (for historical reasons).

Because PRISM uses FORTRAN list directed input for all numeric input, the numeric format is flexible. The formats indicated in the table are suggested formats only. Plus (+) signs are always optional. The variables may be separated by (1) one or more spaces, (2) a comma (,), or (3) a comma and one or more spaces.

Numbered Notes:

1. All records have the same format. PRISM recognizes the end-of-file (eof) mark as an "end-of-data" indicator. Thus the number of records, N, does not have to be specified.
2. PRISM versions through 1.4 ignore F_1 layer parameters. However, future versions *may* make use of these parameters so space is reserved in the input file for them.

Original Document:	2 September 1994	(Version 1.4)	
Revision 1	30 May 1995	(Version 1.5)	(No changes except version number)

TEC (IMS) Input Files for PRISM 1.5
30 May 1995

Record #	Element Name	Data Type	ASCII Format	Units	Description	Repetition Rate	Notes
1...N	YEAR	Integer	XXXX	years	4 digit year of observation	1 per record	1
	DAY	Integer	XXX	days	day of year of observation	1 per record	
	UT	Integer	XXXX	hours and minutes	Universal Time of observation in HHMM format	1 per record	
	GLAT	Real	±XX.XX	degrees	geographic latitude of ionospheric penetration point (IPP)	1 per record	
	GLON	Real	±XXX.XX	degrees	geographic longitude of ionospheric penetration point (IPP)	1 per record	
	TEC	Real	XXX.X	TEC units	vertical equivalent TEC obtained from slant TEC and assigned to IIP	1 per record	2
	OPTIONAL	Character	N/A	N/A	Option descriptive information (e.g., TISS site ID). Ignored by PRISM, may be left blank	1 per record	

General Notes:

The Data Element Names do not necessarily correspond to the FORTRAN variable names in the source code. This is because the FORTRAN names are not always descriptive of the actual contents of the data element (for historical reasons).

Because PRISM uses FORTRAN list directed input for all numeric input, the numeric format is flexible. The formats indicated in the table are suggested formats only. Plus (+) signs are always optional. The variables may be separated by (1) one or more spaces, (2) a comma (,), or (3) a comma and one or more spaces.

Numbered Notes:

1. All records have the same format. PRISM recognizes the end-of-file (eof) mark as an "end-of-data" indicator.
2. The precise definition of the IIP used to calculate the vertical equivalent TEC is not critical as long as it is used consistently.

Original Document	2 September 1994	(Version 1.4)	
Revision 1	30 May 1995	(Version 1.5)	(No changes other than version number)

DMSP Input Files for PRISM 1.5
30 May 1995

File Name: as specified in the Data Control Input File ("PATH_NAM.TXT")

Record #	Element Name	Data Type	ASCII Format	Units	Description	Repetition Rate	Notes
1	HEADER	Character	50 character string	N/A	data identification header: one of 1. "SSIES ION DRIFT" 2. "SSIES IN SITU PLASMA" 3. "SSJ/4 DATA"	1 per data type per satellite	1
2 ("SSIES ION DRIFT")	YEAR	Integer	XXXX	years	4 digit year of observation	1 per record	2,3
	DAY	Integer	XXX	days	day of year of observation	1 per record	
	UT	Integer	XXXXX	seconds	Universal Time of observation	1 per record	
	GLAT	Real	±XX.XX	degrees	geographic latitude of observation	1 per record	
	GLON	Real	±XXX.XX	degrees	geographic longitude of observation	1 per record	
	VV	Real	±X.XXE±XX	$m\ s^{-1}$	vertical ion drift velocity in instrument coordinates	1 per record	
	VH	Real	±X.XXE±XX	$m\ s^{-1}$	horizontal ion drift velocity in instrument coordinates	1 per record	
	EDEN	Real	±X.XXE±XX	cm^{-3}	in situ electron density	1 per record	
2 ("SSIES IN SITU PLASMA")	YEAR	Integer	XXXX	years	4 digit year of observation	1 per record	2,3
	DAY	Integer	XXX	days	day of year of observation	1 per record	
	UT	Integer	XXXXX	seconds	Universal Time of observation	1 per record	
	GLAT	Real	±XX.XX	degrees	geographic latitude of observation	1 per record	
	GLON	Real	±XXX.XX	degrees	geographic longitude of observation	1 per record	
	ALTN	Real	XXXXX.X	km	altitude of spacecraft	1 per record	
	NE	Real	±X.XXE±XX	cm^{-3}	in situ electron density	1 per record	
	TE	Real	±X.XXE±XX	K	in situ electron temperature	1 per record	
	FOP	Real	±X.XXE±XX	N/A	fraction of ions that are O^+	1 per record	
	FHEP	Real	±X.XXE±XX	N/A	fraction of ions that are He^+	1 per record	
	FHP	Real	±X.XXE±XX	N/A	fraction of ions that are H^+	1 per record	
	TI	Real	±X.XXE±XX	K	in situ ion density	1 per record	

Record #	Element Name	Data Type	ASCII Format	Units	Description	Repetition Rate	Notes
2 ("SSJ/4 DATA")	YEAR	Integer	XXXX	years	4 digit year of observation	1 per record	2,3
	DAY	Integer	XXX	days	day of year of observation	1 per record	
	UT	Integer	XXXXX	seconds	Universal Time of observation	1 per record	
	GLAT	Real	±XX.XX	degrees	geographic latitude of spacecraft field line at 110 km	1 per record	4
	GLON	Real	±XXX.XX	degrees	geographic longitude of spacecraft filed line at 110 km	1 per record	4
	EBARE	Real	XXXX.XXX	keV	mean electron energy	1 per record	
	EFLUXE	Real	XXXX.XXX	erg cm^{-2} s^{-1}	energy flux of electrons	1 per record	
	EBARI	Real	XXXX.XXX	keV	mean ion energy	1 per record	
	EFLUXI	Real	XXXX.XXX	erg cm^{-2} s^{-1}	energy flux of protons	1 per record	
	SIGE	Real	XXXX.XXX	erg cm^{-2} s^{-1}	1 sigma uncertainty in EFLUXE	1 per record	
	SIGI	Real	XXXX.XXX	erg cm^{-2} s^{-1}	1 sigma uncertainty in EFLUXI	1 per record	

General Notes:

The Data Element Names do not necessarily correspond to the FORTRAN variable names in the source code. This is because the FORTRAN names are not always descriptive of the actual contents of the data element (for historical reasons).

Because PRISM uses FORTRAN list directed input for all numeric input, the numeric format is flexible. The formats indicated in the table are suggested formats only. Plus (+) signs are always optional. The variables may be separated by (1) one or more spaces, (2) a comma (,), or (3) a comma and one or more spaces.

Numbered Notes:

1. A DMSP input file for PRISM 1.4 may contain three kinds of data, each idenfified by a unique header string:
   "SSIES ION DRIFT" identifies Drift Meter (DM) data
   "SSIES IN SITU PLASMA" identifies data from the Scintillation Meter (SM), Langmuir Probe (EP), and Retarding Potential Analyzer (RPA)
   "SSJ/4 DATA" identifies electron and ion precipitation data
   A DMSP input file may contain data from any number of satellites. However each section, identified by one of the above header strings, may contain data from only one satellite. For example, for a single satellite, there may be at most three sections, one for each kind of data. For two satellites, there may be as many as six sections.
2. The contents of Record 2 depend on the contents of Record 1.
3. This record is repeated until the data of this kind is exhausted. PRISM detects the end of the data by recognizing (1) the EOF mark, or (2) encountering a new header string.
4. Because precipitating electrons and ions are constrained to move along magnetic field lines, and because PRISM is trying to determine the effects in the auroral E-layer near 110 km altitude, the desired coordinates are the geographic location of the geomagnetic field line that passes through the spacecraft at 110 km instead of the actual location of the spacecraft.

Original document:	27 September 1994		
Revision 1:	5 October 1994	(record 1; record 2, "SSJ/4 DATA"; and note 4)	
Revision 2:	30 May 1995	(Version 1.5)	(no changes except version number)

Output Station List Input File for PRISM 1.5
30 May 1995

Record #	Element Name	Data Type	ASCII Format	Units	Description	Repetition Rate	Notes
1...N	GLAT	Real	±XX.XX	degrees	geographic latitude of ionosonde	1 per record	1
	GLON	Real	±XXX.XX	degrees	geographic longitude of ionosonde	1 per record	
	OPTIONAL	Character	N/A	N/A	Optional information (e.g., WMO number): ignored by PRISM, may be left blank	1 per record	

General Notes:

The Data Element Names do not necessarily correspond to the FORTRAN variable names in the source code. This is because the FORTRAN names are not always descriptive of the actual contents of the data element (for historical reasons).

Because PRISM uses FORTRAN list directed input for all numeric input, the numeric format is flexible. The formats indicated in the table are suggested formats only. Plus (+) signs are always optional. The variables may be separated by (1) one or more spaces, (2) a comma (,), or (3) a comma and one or more spaces.

Numbered Notes:

1. All records have the same format. PRISM recognizes the end-of-file (eof) mark as an "end-of-data" indicator. Thus the number of records, N, does not have to be specified.

Original Document 2 September 1994
Revision 1: 30 May 1995 (Version 1.5) (No changes other than version number)

Gridded Output Specification for PRISM 1.5
30 May 1995

File Name: as specified in PRISM Input Stream

Record #	Element Name	Data Type	ASCII Format	Units	Description	Repetition Rate	Notes
1	Header	Character	" YEAR DAY ..."	N/A	column labels for numeric data in record 2	1 per file	
2	Separator	Character	"--------..."	N/A	separator (row of hyphens)	1 per file	
3	YEAR	Integer	XXXX	N/A	4 digit year (e.g., 1989)	1 per file	
	DAY	Integer	XXX	N/A	day of year (1 Jan = 001, etc.)	1 per file	
	UT	Real	XXXXX.X	seconds	Universal Time	1 per file	
	F10P7	Real	XXX.X	solar flux units	Solar radio flux at 10.7 cm (2800 Mhz) (daily value)	1 per file	
	RKP	Real	XX.X	N/A	Kp geomagnetic activity index	1 per file	
	SSN	Real	XXXX.X	N/A	Solar Sunspot Number	1 per file	
4	blank line	N/A	N/A	N/A	blank line	1 per file	
5	blank line	N/A	N/A	N/A	blank line	1 per file	
6	IGM	Integer	X	N/A	flag indicating coordinate system: 0 = geomagnetic, 1 = geographic	1 per file	
7	Header	Character	" Latitude Longitude ..."	N/A	header for grid information	1 per file	
8	Header	Character	" Starting Ending ..."	N/A	subheader for grid information	1 per file	

Record #	Element Name	Data Type	ASCII Format	Units	Description	Repetition Rate	Notes
9	LAT0	Real	XXXX.XX	degrees	starting latitude of grid (southwest corner)	1 per file	
	LATF	Real	XXXX.XX	degrees	ending latitude of grid (northeast corner)	1 per file	
	LON0	Real	XXXX.XX	degrees	starting longitude of grid (southwest corner)	1 per file	
	LONF	Real	XXXX.XX	degrees	ending longitude of grid (northeast corner)	1 per file	
	NUMLAT	Integer	XXXXXX	N/A	number of latitude points in grid	1 per file	
	NUMLON	Integer	XXXXXX	N/A	number of longitude points in grid	1 per file	
	DLAT	Real	XXXX.XX	degrees	latitude spacing	1 per file	
	DLON	Real	XXXX.XX	degrees	longitude spacing	1 per file	
10	IOUT	Integer	XX	N/A	indicator for type of output at each grid point: 0 = profile parameters (critical frequencies and heights) only 1 = electron density profiles only 2 = both electron density profiles and profile parameters	1 per file	1

Record #	Element Name	Data Type	ASCII Format	Units	Description	Repetition Rate	Notes
11 (IOUT=0)	blank line	N/A	N/A	N/A	blank line	1 per record	2
12 (IOUT=0)	GGLAT	Real	XXXX.XX	degrees	geographic latitude of grid point	1 per record	2
	GGLON	Real	XXXX.XX	degrees	geographic longitude of grid point	1 per record	
	MLAT	Real	XXXX.XX	degrees	geomagnetic latitude of grid point	1 per record	
	MLON	Real	XXXX.XX	degrees	geomagnetic longitude of grid point	1 per record	
	MLT	Real	XX.XX	hours	geomagnetic local time	1 per record	
13 (IOUT=0)	FOF2	Real	XXXX.XX	MHz	critical frequency of F2 layer	1 per record	2
	HMF2	Real	XXXX.XX	km	height of F2 layer	1 per record	
	FOF1	Real	XXXX.XX	MHz	critical frequency of F1 layer	1 per record	8
	HMF1	Real	XXXX.XX	km	height of F1 layer	1 per record	8
	FOE	Real	XXXX.XX	Mhz	critical frequency of E layer	1 per record	
	HME	Real	XXXX.XX	km	height of E layer	1 per record	
	TEC	Real	XXX.X	TEC units	Total Electron Content	1 per record	7

Record #	Element Name	Data Type	ASCII Format	Units	Description	Repetition Rate	Notes
11 (IOUT=1)	label	Character	"Number of altitude points = '	N/A	label for numeric element NALT	1 per file	3
	NALT	Integer	XXXXXX	N/A	number of altitudes on grid	1 per file	
12 (IOUT=1)	Header	Character	"Altitudes"	N/A	header for list of altitude grid	1 per file	3
13 (IOUT=1)	ALT	Real	XXXX.XX	km	altitude of a point on the altitude grid	5 per record	4
14 (IOUT=1)	blank line	N/A	N/A	N/A	blank line	1 per record	5
15 (IOUT=1)	GGLAT	Real	XXXX.XX	degrees	geographic latitude of grid point	1 per record	5
	GGLON	Real	XXXX.XX	degrees	geographic longitude of grid point	1 per record	
	MLAT	Real	XXXX.XX	degrees	geomagnetic latitude of grid point	1 per record	
	MLON	Real	XXXX.XX	degrees	geomagnetic longitude of grid point	1 per record	
	MLT	Real	XX.XX	hours	geomagnetic local time	1 per record	
16 (IOUT=1)	Header	Character	" Densities"	N/A	header for electron densities	1 per record	5
17 (IOUT=1)	EDEN	Real	±X.XXE±XX	cm^{-3}	electron density corresponding to altitude in record 11	5 per record	4,5

Record #	Element Name	Data Type	ASCII Format	Units	Description	Repetition Rate	Notes
11 (IOUT=2)	Label	Character	"Number of altitude points = '	N/A	label for numeric element NALT	1 per file	3
	NALT	Integer	XXXXXX	N/A	number of altitudes on grid	1 per file	3
12 (IOUT=2)	Header	Character	"Altitudes"	N/A	header for list of altitude grid	1 per file	3
13 (IOUT=2)	ALT	Real	XXXX.XX	km	altitude of a point on the altitude grid	5 per record	4
14 (IOUT=2)	blank line	N/A	N/A	N/A	blank line	1 per record	6
15 (IOUT=2)	GGLAT	Real	XXXX.XX	degrees	geographic latitude of grid point	1 per record	6
	GGLON	Real	XXXX.XX	degrees	geographic longitude of grid point	1 per record	
	MLAT	Real	XXXX.XX	degrees	geomagnetic latitude of grid point	1 per record	
	MLON	Real	XXXX.XX	degrees	geomagnetic longitude of grid point	1 per record	
	MLT	Real	XX.XX	hours	geomagnetic local time	1 per record	
16 (IOUT=2)	Header	Character	" Densities"	N/A	header for electron densities	1 per record	6
17 (IOUT=2)	EDEN	Real	±X.XXE±XX	cm^{-3}	electron density corresponding to altitude in record 11	5 per record	4,6
18 (IOUT=2)	Header	Character	" foF2 hmF2 ..."	N/A	header for profile parameters	1 per record	6
19 (IOUT=2)	FOF2	Real	XXXX.XX	MHz	critical frequency of F2 layer	1 per record	6
	HMF2	Real	XXXX.XX	km	height of F2 layer	1 per record	
	FOF1	Real	XXXX.XX	MHz	critical frequency of F1 layer	1 per record	8
	HMF1	Real	XXXX.XX	km	height of F1 layer	1 per record	8
	FOE	Real	XXXX.XX	Mhz	critical frequency of E layer	1 per record	
	HME	Real	XXXX.XX	km	height of E layer	1 per record	
	TEC	Real	XXX.X	TEC units	Total Electron Content	1 per record	7

Notes:

1. The structure of the PRISM gridded output file after Record 10 depends on the content of Record 10.
2. For IOUT=0, Records 11-13 are repeated until the data for every grid point has been written.
3. For IOUT=1 or 2, Records 11 and 12 are written only once.
4. This Record is repeated until the contents of the Data Element have been exhausted.
5. For IOUT=1, Records 14-17 are repeated until the data for every grid point has been written.
6. For IOUT=2, Records 14-19 are repeated unitl the data for every grid point has been written.
7. 1 TEC unit = 10^{12} cm^{-2} = 10^{16} m^{-2}
8. PRISM 1.4 does not currently calculate F_1 layer parameters, but future versions may do so.

Original document:	2 September 1994
revision 1:	6 September 1994 (record 13, IOUT=0; record 19, IOUT=2)
revision 2:	26 September 1994 (record 13, IOUT=0; record 13, IOUT=1 & 2; record 19, IOUT=2; Notes 6 & 8)
revision 3:	10 November 1994 (record 12, IOUT=0, record 15, IOUT=1 & 2)
revision 4:	30 May 1995 (Version 1.5) (No changes other than version number)

"Station" Output Specification for PRISM 1.5
30 May 1995

File Name: TMPA.DAT

Record #	Element Name	Data Type	ASCII Format	Units	Description	Repetition Rate	Notes
1	DTYPE	Character	" IONOSONDE "	N/A	identifies data type	1 per record	
	text	Character	" data "	N/A		1 per record	
	NRECL	Integer	XXX	N/A	number of output station sites	1 per record	
	text	Character	" records"	N/A		1 per record	
2	IOUTS	Integer	X	N/A	indicator for type of output at each station: 0 = profile parameters only 1 = electron density profiles only 2 = both profile parameters and electron density profiles 3 = no output at station sites	1 per file	1

Record #	Element Name	Data Type	ASCII Format	Units	Description	Repetition Rate	Notes
3 (IOUTS=0)	Header	Character	" NUM UT..."	N/A	column labels	1 per file	
4 (IOUTS=0)	NUM	Integer	XXX	N/A	site number	1 per record	2
	UT	Real	XX.XX	hours	UT (decimal hours)	1 per record	
	LAT	Real	±XX.XX	degrees	geographic latitude	1 per record	
	LON	Real	±XXX.XX	degrees	geographic longitude	1 per record	
	MLAT	Real	±XX.XX	degrees	geomagnetic latitude	1 per record	
	MLON	Real	±XXX.X	degrees	geomagnetic longitude	1 per record	
	MLT	Real	XX.XX	hours	geomagnetic local time	1 per record	
	FOF2	Real	XX.XX	MHz	critical frequency of F2 layer	1 per record	
	HMF2	Real	XXX.XX	km	height of F2 layer	1 per record	
	FOF1	Real	XX.XX	MHz	critical frequency of F1 layer	1 per record	3
	HMF1	Real	XXX.XX	km	height of F1 layer	1 per record	3
	FOE	Real	XX.XX	MHz	critical frequency of E layer	1 per record	
	HME	Real	XXX.XX	km	height of E layer	1 per record	
	TEC	Real	XXX.X	TEC units	vertical TEC	1 per record	7

Record #	Element Name	Data Type	ASCII Format	Units	Description	Repetition Rate	Notes
3 (IOUTS=1)	label	Character	"Number of altitude points = "	N/A	label for numberic element NALT	1 per file	
	NALT	Integer	XXXXXX	N/A	number of altitudes on altitude grid	1 per file	
4 (IOUTS=1)	Header	Character	"Altitudes"	N/A	header for list of altitude grid	1 per file	
5 (IOUTS=1)	ALT	Real	XXXX.XX	km	altitude of a point on the altitude grid	5 per record	4
6 (IOUTS=1)	blank line	N/A	N/A	N/A	blank line	1 per record	5
7 (IOUTS=1)	NUM	Real	XXX	N/A	site number		
	UT	Real	XX.XX	hours	Universal Time (decimal hours)		
	LAT	Real	±XXX.XX	degrees	geographic latitude		
	LON	Real	±XXX.XX	degrees	geographic longitude		
	MLAT	Real	±XXX.XX	degrees	geomagnetic latitude		
	MLON	Real	±XXX.XX	degrees	geomagnetic longitude		
	MLT	Real	XXXX.XX	decimal hours	geomagnetic local time		
8 (IOUTS=1)	Header	Character	" Densities"	N/A	header for electron densities	1 per record	5
9 (IOUTS=1)	EDEN	Real	±X.XXE±XX	cm^{-3}	electron density corresponding to altitude grid in record 4	5 per record	4,5

Record #	Element Name	Data Type	ASCII Format	Units	Description	Repetition Rate	Notes
3 (IOUTS=2)	Label	Character	"Number of altitude points = '	N/A	label for numeric element NALT	1 per file	
	NALT	Integer	XXXXXX	N/A	number of altitudes on grid	1 per file	
4 (IOUTS=2)	Header	Character	"Altitudes"	N/A	header for list of altitude grid	1 per file	
5 (IOUTS=2)	ALT	Real	XXXX.XX	km	altitude of a point on the altitude grid	5 per record	4
6 (IOUTS=2)	blank line	N/A	N/A	N/A	blank line	1 per record	6
7 (IOUTS=2)	NUM	Integer	XXX	N/A	site number	1 per record	6
	UT	Real	XX.XX	hours	UT (decimal hours)	1 per record	
	LAT	Real	±XX.XX	degrees	geographic latitude	1 per record	
	LON	Real	±XXX.XX	degrees	geographic longitude	1 per record	
	MLAT	Real	±XX.XX	degrees	geomagnetic latitude	1 per record	
	MLON	Real	±XXX.X	degrees	geomagnetic longitude	1 per record	
	MLT	Real	XX.XX	hours	geomagnetic local time	1 per record	
	FOF2	Real	XX.XX	MHz	critical frequency of F2 layer	1 per record	
	HMF2	Real	XXX.XX	km	height of F2 layer	1 per record	
	FOF1	Real	XX.XX	MHz	critical frequency of F1 layer	1 per record	3
	HMF1	Real	XXX.XX	km	height of F1 layer	1 per record	3
	FOE	Real	XX.XX	MHz	critical frequency of E layer	1 per record	
	HME	Real	XXX.XX	km	height of E layer	1 per record	
	TEC	Real	XXX.X	TEC units	vertical TEC	1 per record	7
8 (IOUTS=2)	Header	Character	" Densities"	N/A	header for electron densities	1 per record	
9 (IOUTS=2)	EDEN	Real	±X.XXE±XX	cm^{-3}	electron density corresponding to altitude in record 11	5 per record	4

Notes:

1. The structure of the PRISM station output file after Record 2 depends on the content of Record 2.
2. For IOUTS=0, Record 4 is repeated NRECL times.
3. PRISM 1.4 does not actually compute F1 layer parameters, but future versions may do so.
4. This record is repeated until the contents of the data element have been exhausted.
5. For IOUTS=1, Records 6-9 are repeated NRECL times.
6. For IOUTS=2, Records 6-11 are repeated NRECL times.
7. 1 TEC unit = 10^{12} cm^{-2} = 10^{16} m^{-2}

Original document:	2 September 1994	
revision 1:	26 September 1994 (records 2, and 3-11; notes 4-7)	
revision 2:	3 November (File Name, on first page)	
revision 3:	30 May 1995 (Version 1.5)	(No changes other than version number)

References

Anderson, D. N., A theoretical study of the ionospheric *F*-region equatorial anomaly, II, Results in the American and Asian sectors,*Planet. Space. Sci.*, **21**, 421-442, 1973.

Bailey, G. J., and R. Sellek, A mathematical model of the Earth's plasmasphere and its application in a study of He^+ at L = 3, *Ann. Geophys.*, *8*, 171,1990.

Beckmann, P., *Orthogonal Polynomials for Engineers and Physicists*, The Golem Press, Boulder, pp. 91-92, 1973.

Brace, L. H., and R. F. Theis, Global empirical models of ionospheric electron temperature in the upper F-region and plasmasphere based on in situ measurements from the Atmosphere Explorer-C, ISIS 1, and ISIS 2 satellites, *J. Atmos. Terr. Phys.*, *43*, 1317, 1981.

Daniell, R. E., W. G. Whartenby, and L. D. Brown, *PRISM Validation*, PL-TR-94-2198, Phillips Laboratory, Hanscom AFB, Massachusetts, 1994, **ADA288476**

Davis, R. E., Predictability of Sea Surface Temperature and Sea Level Pressure Anomalies Over the North Pacific Ocean, *J. Phys. Oceanogr.*, 6, 249, 1976.

Decker, D. T., C. E. Valladares, R. Sheehan, Su. Basu, D. N. Anderson, and R. A. Heelis, Modeling daytime*F* layer patches over Sondrestrom, *Radio Sci.*, *29*, 249-268, 1994.

Fejer, B. G., The equatorial ionospheric electric fields, A review, *J. Atmos. Terr. Phys.*, *43*, 377-386, 1981.

Fejer, B. G., E. R. de Paula, I. S. Batista, E. Bonelli, and R. F. Woodman, Equatorial *F* region vertical plasma drifts during solar maxima,*J. Geophys. Res.*, *94*, 12049-12054, 1989.

Fejer, B. G., E. R. de Paula, R. A. Heelis, and W. B. Hanson, Global equatorial ionospheric vertical plasma drifts measured by the AE-E satellite, *J. Geophys. Res.*, *100*, 5769-5776, 1995.

Gussenhoven, M. S., D. A. Hardy, and N. Heinemann, Systematics of the equatorward diffuse auroral boundary, *J. Geophys. Res.*, *88*, 5692-5708, 1983.

Hardy, D. A., M. S. Gussenhoven, R. R. Raistrick, and W. J. McNeil, Statistical and functional representations of the pattern of auroral energy flux, number flux, and conductivity, *J. Geophys. Res.*, 92, 12275-12294, 1987.

Hedin, A. E., MSIS-86 Thermospheric Model, *J. Geophys. Res.*, 92, 4649-4662, 1987.

Hedin, A. E., Empirical global model of upper thermosphere winds based on Atmospheric and Dynamics Explorer satellite data, *J. Geophys. Res.*, *93*, 9959-9978, 1988.

Heppner, J. P., and N. C. Maynard, Empirical high-latitude electric field models, *J. Geophys. Res.*, *92*, 4467-4489, 1987.

Hildebrand, F. B., *Methods of Applied Mathematics*, Prentice-Hall, Englewood Cliffs, pp. 30-34, 1965.

Jasperse, J. R., The photoelectron distribution function in the terrestrial ionosphere, in *Physics of Space Plasmas*, ed. by T. S. Chang, B. Coppi, and J. R. Jasperse, Scientific Publishers, Cambridge, MA, pp. 53-84, 1982.

Kutzbach, J. E., Empirical Eigenvectors of Sea-Level Pressure, Surface Temperature, and Precipitation Complexes over North America, *J. Appl. Meteor.*, 6, 791, 1967.

Lorenz, E. N., *Empirical Orthogonal Functions and Statistical Weather Prediction*, Sci. Rep. No. 1, Contract AF19(604)1566, AFCRC-TN-57-256, Dept. Meteor., MIT, 1956.

Moffett, R. J., The equatorial anomaly in the electron distribution of the terrestrial F-region, *Fundamentals of Cosmic Phys.*, 4, 313-391, 1979.

Peixota, J. P., and A. H. Oort, *Physics of Climate*, Appendix B, American Institute of Physics, New York, 1991.

Schunk, R. W., A Mathematical Model of the Middle and High Latitude Ionosphere, *Pageoph*, 127, 255-303, 1988.

Secan, J. A., and T. F. Tascione, The 4D Ionospheric Objective Analysis Model, in *Proceedings of the 1984 Ionospheric Effects Symposium*, ed. by Goodman, Klobuchar, and Soicher, 336-345, 1984.

Strickland, D. J., D. L. Book, T. P. Coffey, and J. A. Fedder, Transport equation techniques for the deposition of auroral electrons, *J. Geophys. Res.*, **81**, 2755-2764, 1976.

Strickland, D. J., R. E. Daniell, J. R. Jasperse, and B. Basu, Transport-theoretic model for the electron-proton-hydrogen atom aurora: 2. Model results, in press, *J. Geophys. Res.*, 1994.

Tascione, T. F., H. W. Kroehl, R. Creiger, J. W. Freeman, R. A. Wolf, R. W. Spiro, R. V. Hilmer, J. W. Shade, and B. W. Hausman, New ionospheric and magnetospheric specification models, *Radio Science*, *23*, 211-222, 1988.